Environmental Science
Water Research & Technology

ROYAL SOCIETY OF CHEMISTRY

CRITICAL REVIEW

View Article Online
View Journal | View Issue

Cite this: *Environ. Sci.: Water Res. Technol.*, 2020, **6**, 258

Capacitive deionization and electrosorption for heavy metal removal

Raylin Chen, Thomas Sheehan, Jing Lian Ng, Matthew Brucks and Xiao Su *

Received 22nd October 2019,
Accepted 6th December 2019

DOI: 10.1039/c9ew00945k

rsc.li/es-water

Capacitive deionization (CDI) technologies have gained intense attention for water purification and desalination in recent years. Inexpensive and widely available porous carbon materials have enabled the fast growth of electrosorption research, highlighting the promise of CDI as a potentially cost-effective technology to remove ions. Whereas the main focus of CDI has been on bulk desalination, there has been a recent shift towards electrosorption for selective ion separations. Heavy metals are pollutants that can have severe health impacts and are present in both industrial wastewater and groundwater leachates. Heavy metal ions, such as chromium, cadmium, or arsenic, are of great concern to traditional treatment technologies, due to their low concentration and the presence of competing species. The modification/functionalization of porous carbon and recent developments of faradaic and redox-active materials have offered a new avenue for selective ion-binding of heavy metal contaminants. Here, we review the progress in electrosorptive technologies for heavy metal separations. We provide an overview of the wide applicability of carbon-based electrodes for heavy metal removal. In parallel, we highlight the trend toward modification of carbon materials, new developments in faradaic interfaces, and the underlying physico-chemical mechanisms that promote selective heavy metal separations.

Water impact

Heavy metals are highly toxic, and exposure to contaminated water threatens millions of people around the world. Capacitive deionization (CDI) and electrosorption have shown promise as cost and energy-efficient methods to desalinate and deionize water. Developing efficient CDI methods to remove heavy metal ions can be an effective approach for more sustainable water treatment and purification.

1. Introduction

There is no formal definition for "heavy metals"; the term broadly refers to metals with high density or atomic weights.[1] Heavy metals present an environmental concern because they are hazardous to human health, even at trace concentrations, with effects ranging from acutely toxic to carcinogenic after chronic exposure.[2] Heavy metal contamination originates from both natural and anthropogenic sources. Millions of people are exposed to contaminated soil and drinking water, where naturally occurring heavy metals in rock and sediment leach into water sources.[3] Even in regions with clean drinking water, heavy metal exposure can continue to be a problem through contaminated food.[4] These toxic compounds are continuously discharged into the environment from industries such as electronic-circuit production, steel and other metal processing, and fine-chemical production. Heavy metal toxicity is worsened as heavy metals move up the food chain and bioaccumulate in living organisms.[5,6]

Conventional processes for heavy metal removal, such as chemical precipitation and coagulation–flocculation, struggle with selectively removing heavy metals, and produce large quantities of toxic solid sludge.[6] Processes that are typically used for desalination can, in principle, be used to remove heavy metal ions, but they may become inefficient because heavy metal contamination exists at much lower concentrations than typical salts.[7] Amidst research into novel ways to remove metals, such as various membrane,[8,9] bioelectrochemical,[10] and photocatalytic processes,[11,12] electrosorption processes are emerging as an efficient and facile way to remove heavy metals and other ions from water.[13–15]

Electrosorption refers to adsorption of a dissolved species onto an electrode, with the surface binding promoted by an electric field.[16] A typical electrosorption cell consists of two electrodes sandwiching a feed of water (Fig. 1a). Electrosorption is induced by polarizing the electrodes with

Department of Chemical and Biomolecular Engineering, University of Illinois at Urbana-Champaign, Urbana, Illinois 61801, USA. E-mail: x2su@illinois.edu

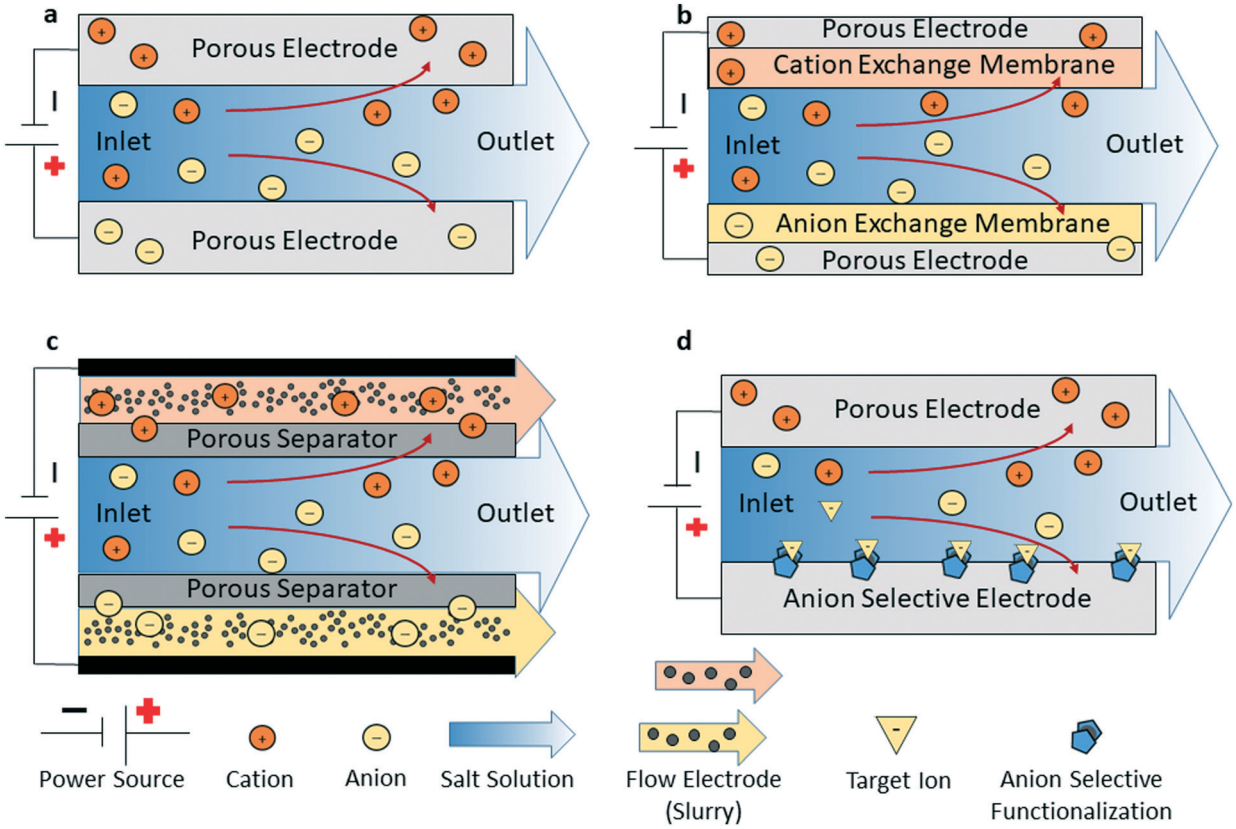

Fig. 1 Schematic of various CDI and electrosorption processes. (a) A flow-by CDI cell with two porous electrodes sandwiching a feed of water. A potential difference applied across the two electrodes polarizes the electrodes and induces electrosorption of ions. Electrosorption processes are modular and (b) can be combined with membrane processes or (c) operated with flow electrodes. (d) Recent trends in electrosorption focus on designing materials that can selectively remove target ions.

an applied voltage bias. Traditionally, electrodes for electrosorption are made of conductive, non-Faradaic materials such as porous carbon. During charging, in order to satisfy charge neutrality, ions of opposite charge are attracted to the polarized electrode by coulombic forces and electric charge is built up at the surface of the electrode, much like in an electric capacitor. At the surface of the polarized electrode, the ions form an electric double-layer.[17] Utilizing this phenomenon to remove ions from solution is referred to as capacitive deionization (CDI). Ions are held in the double layer until the applied bias is stopped or reversed to discharge the electrodes. Upon discharge, the ions are liberated and the electrodes are regenerated. Because the CDI process stores charge, the energy used in an electrosorption process can partially be recovered, making them possibly more energy efficient than other ion removal techniques.[18] Electrosorption research has expanded to include Faradaic (or redox active) materials as electrodes. When using redox active materials,ions are captured to neutralize the change imbalance created by the redox reaction, as opposed to capturing ions in an electric double layer. Redox reactions involving the removal (or addition) of an electron from the electrode demand the addition of a anion (or cation) to satisfy charge neutrality. This process is sometimes referred to as electrochemical ion exchange. While the physical phenomena is slightly different, operation of electrosorption *via* electrochemical ion exchange is the same as with CDI. Regeneration of the electrode occurs when the opposite bias is applied, reversing the redox reaction and expelling the ions. Examples of electrode materials for electrochemical ion exchange include polyvinylferrocene and polypyrrole.[19,20] Other redox materials that can remove metal ions are ion intercalation electrodes. These materials incorporate metal ions into the electrode crystalline structure though a redox reaction. While more commonly used as electrodes for batteries,[21] a few of these materials have also been used for heavy metal ion removal. Electrosorptive and capacitive deionization processes are modular and can be combined with other ion removal technologies such as membranes,[22–25] ion-exchange resins,[26] and microbial desalination techniques[27] to improve efficiencies and leverage the advantages of the individual processes.

CDI research has focused on water desalination, and has emerged as an energy and cost efficient method for removing salt at low concentrations from water.[28] Materials such as activated carbon (AC) have frequently been used in CDI studies because they are inexpensive and have high specific surface areas. CDI is most effective when the electrode has a

high specific surface area, enabling much of the electrode material to participate in double-layer formation. While porous carbon materials are great for indiscriminately capturing all ionic species from water, electrosorption research is moving toward designing materials that can selectively remove certain ions of interest from competing ions.[29–31]

This review provides an overview of recent and current research on electrosorption/CDI for As, Cd, Cr, Cu, Fe, Ni, Pb, V, U, Zn. In addition to porous carbon materials, we also focus on recent studies of surface modification of carbon, which can be used to control ion selectivity, as well as non-carbon materials that are being engineered to enhance ion selectivity and uptake capacity.

2. Heavy metal electrosorption

2.1 Arsenic

While technically a metalloid, arsenic is often grouped with heavy metals because of its similar density and toxicity. Arsenic is a toxic and carcinogenic element that can cause skin lesions, vomiting, diarrhea, convulsions, and death.[3] Arsenic is primarily released into the environment from arsenic-enriched minerals, and drinking water contaminated with arsenic threatens over 100 million people in Bangladesh, Cambodia, China, India, Laos, Myanmar, Nepal, Pakistan, Taiwan, and Vietnam.[32] The World Health Organization (WHO) recommended limit of arsenic in drinking water is 10 μg L^{-1} and the United States Environmental Protection Agency (EPA) Maximum Contaminant Level (MCL) for arsenic is also 10 μg L^{-1}.[33,34]

Arsenic is most commonly found in the +3 and +5 oxidation states, with As(III) being more toxic than As(V).[35,36] Under oxidizing conditions and at slightly acidic pH values, inorganic arsenic is most commonly found in the pentavalent form as $H_2AsO_4^-$. At higher pH values, this becomes $HAsO_4^{2-}$. In reducing conditions and at pH values below 9.2, arsenic is generally found in the +3 oxidation state as the neutral species H_3AsO_3.[37] During As(III) electrosorption, it is common for As(III) to be oxidized to As(V) at the anode.[38,39]

Arsenic electrosorption studies have focused on AC electrodes (Table 1). The As uptake of AC electrodes can be enhanced when combined with other materials to make composite electrodes. Recently, redox-active polymer, poly(vinylferrocene), has been shown to be an extremely selective adsorbent for As electrosorption.[40]

2.1.1 Activated carbon electrodes. Electrosorption using electrodes made from wood AC powder (Sinopharm Chemical Reagent Company, China) removed As(III) and simultaneously oxidized As(III) into As(V) at the anode.[38] The amount of As(III) that was oxidized increased with pH, but the adsorption As declined in highly alkaline solutions (pH > 11) due to competition from OH^- ions. These wood AC powder electrodes removed 4.73 mg As per g AC (4.73 mg g^{-1}) from a 1 mmol L^{-1} As (75 mg L^{-1}) solution at 1.0 V. Commercially available granular AC Darco 1220 removed 0.066 mg As per g AC at 1.0 V and 0.3 mg g^{-1} at 1.5 V from a 100 μg L^{-1} As and 500 mg L^{-1} NaCl solution.[41] When 100 μg L^{-1} Cr was added to these 100 μg L^{-1} As solutions, the arsenic uptake was enhanced. This enhanced uptake was likely due to the formation of an insoluble As–Cr compound because As and Cr were removed in a 1 : 1 molar ratio.

Around pH 6, AC (Filtrasorb 400, Chemviron Carbon Inc.) electrodes have a higher capacity for As(V) (10.31 mg g^{-1}) than for As(III) (7.57 mg g^{-1}) when adsorbing As from a 200 mg L^{-1} solution at a 1.2 V potential.[39] The lower adsorption uptake

Table 1 Arsenic

Species	Electrode material	Specific surface area (m^2 g^{-1})	Voltage/charge	Initial concentration	Percent of heavy metal removed	Electrosorption capacity (mg g^{-1})	Operation time	pH	Ref.
As(III, V)	Granular activated carbon (AC)	650	1.0 V	100 μg L^{-1}	16%	0.066	25.3 h	4.5	41
			1.5 V	100 μg L^{-1}	83.2%	0.337	18.6 h		
As(V)	Granular AC	880 (BET)	1.5 V	~55 μg L^{-1}	~50%	0.0031	24 h	8.2	42
As(III)	Wood AC powder	—	1.0 V	1 mmol L^{-1} (75 mg L^{-1})	—	4.73	45 min		38
As(V)	AC	1396.11	1.2 V	10 mg L^{-1}	—	~6.5	120 min	—	43
	Reduced graphene–iron composite (Fe–rGO)	247.34	1.2 V	10 mg L^{-1}	—	~14	240 min	—	
	Fe–rGO@AC	—	1.2 V	10 mg L^{-1}	—	~10	120 min	—	
As(III, V)	AC	964	1.2 V	0.13 mg L^{-1}	77%	0.002	50 min	—	44
As(V)	AC	964	1.2 V	200 mg L^{-1}	—	10.31			39
As(III)	AC	964	1.2 V	200 mg L^{-1}	—	7.57			
As(V)	AC-poly(vinylidene fluoride)		2.0 V	1 mg L^{-1}	98.8%	—		9	45
As(V)	AC fiber	121.11	1.5 V	—	—	4.05 (Langmuir fit maximum)			46
	TiO_2–AC fiber	71.63	1.5 V	—	—	8.09 (Langmuir fit maximum)			
As(V)	Poly(vinylferrocene)	—	0.8 V *vs.* Ag/AgCl	1 mM (75 mg L^{-1})	—	~75	—	5	40

for As(III) may have been because around pH 6, As(V) exists predominantly as anionic $H_2AsO_4^-$, while As(III) exists predominantly as neutral H_3AsO_3 and therefore a large fraction of As(III) was not electrostatically attracted to either electrode. In order for uncharged As(III) species to be electrosorbed, they needed to be oxidized at the anode to anionic As(V). The adsorption capacity of these Filtrasorb 400 AC electrodes decreased significantly when NaCl or natural organic matter (NOM, humic acid, Aldrich) was added to the arsenic containing solution. Negative Cl^- ions and negatively charged NOM compete with arsenic for adsorption sites. Finally, it was also shown that Filtrasorb 400 AC electrodes were effective at removing arsenic from contaminated ground water and decreased the As concentration from 0.13 mg L^{-1} to 0.03 mg L^{-1} from a sample of As-contaminated ground water.[44]

2.1.2 Carbon-based composite electrodes. The arsenic adsorption capacity of AC electrodes can be greatly enhanced when combined with other materials to make composite electrodes. The addition of TiO_2 to AC fiber felt electrodes raised the adsorption capacity from 4.05 mg g^{-1} As (for the felt alone) to 8.09 mg As per g (Langmuir fit maximum) at 1.5 V despite the decrease in specific surface area for the TiO_2–AC, as noted in Table 1.[46] Electrodes made of AC and reduced graphene–iron composite (Fe–rGO) removed 13.00 mg g^{-1} As from a 10 mg L^{-1} solution at 1.2 V.[43] Without the Fe–rGO, the AC alone removed just 6.57 mg g^{-1}. Composite electrodes containing AC powder and poly(vinylidene fluoride) removed 98.80% of the arsenic from a 1 mg L^{-1} solution upon the application of a 2 V potential.[45] This 98.8% removal lowered the final concentration to 0.012 mg L^{-1}, very close to WHO and US EPA standards.

Films containing carbon nanotubes (CNTs) and redox-active polymer poly(vinylferrocene) were able to adsorb about 75 mg g^{-1} As from a 1 mM As(V) (75 mg L^{-1}), 20 mM NaCl (1169 mg L^{-1}) solution upon the application of a 0.8 V *vs.* Ag/AgCl potential.[40] Rather than holding As ions in an electric double-layer, poly(vinylferrocene), when oxidized, binds to arsenic oxyanions through charge transfer between the positive ferrocenium units and the negative oxyanions. Arsenic anions were selectively adsorbed over competing Cl^- ions because the arsenic anions were more polarizable than Cl^- and transferred more charge to the oxidized poly(vinylferrocene) resulting in a higher binding energy for arsenic anions than for Cl^-.

2.2 Cadmium

Chronic cadmium exposure is associated with kidney disease, osteoporosis, cardiovascular disease, and cancer.[47,48] Cadmium contamination and exposure is most prevalent in Asian countries such as China, Japan, Thailand, and Sri Lanka.[49–51] Many people in these countries irrigate rice paddies using river water downstream from industrial sites, where cadmium-containing ore is refined for electronic devices and batteries. As a result, cadmium builds up in the rice and other crops, and cadmium exposure occurs through consumption of these crops.[47,52] In Jiangxi Province, China, researchers from the World Health Organization have determined that 99.5% of the residents' cadmium intake originated locally grown crops due to the presence of tungsten ore processing plants upstream from farming communities.[49] The WHO guideline value for Cd in drinking water is 3 μg L^{-1} and the US EPA MCL for Cd in drinking water is 5 μg L^{-1}.[34,53] Various electrode materials used for Cd electrosorption are listed in Table 2.

2.2.1 Carbon-based electrodes. AC cloth (ACC, FM70) electrodes removed 31.85% of the Cd^{2+} present in a 0.5 mM Cd^{2+} (56.2 mg L^{-1}) solution at pH 3.8 and 1.2 V.[13] In competitive adsorption experiments, with the addition of 0.5 mM Cr^{3+} (26 mg L^{-1}) and 0.5 mM Pb^{2+} (104 mg L^{-1}), these FM70 ACC electrodes struggled to remove Cd. The Cd removal efficiency dropped from 31.85% in the individual removal experiment to 13.57% in the competitive removal experiment. Meanwhile, the removal efficiency for Cr only dropped from 52.48% to 46.22% and the removal efficiency for Pb increased from 42.62% to 45.53% between the individual heavy metal removal experiments and the competitive removal experiment. Among the Cd, Cr, and Pb individual removal tests, Cd electrosorption showed the lowest electrosorption rate. Cd^{2+} electrosorption was hypothesized to be slower than Pb^{2+} and Cr^{3+} due to its hydraulic radius and charge. Ions with higher charge and smaller hydraulic radius are preferred in adsorption.[13] Among the three ions, Pb^{2+} has the smallest hydraulic radius ($Pb^{2+} < Cd^{2+} < Cr^{3+}$) which allowed it to be adsorbed quickly. While Cr^{3+} has the largest hydraulic radius, it adsorbed quickly because it has a higher charge than Pb^{2+} and Cd^{2+}. The combination of these two effects may have caused Cd^{2+} to be out competed by the other ions in the competitive removal experiment. Carbon aerogels removed 97.5% of the Cd from a 200 mg L^{-1} solution at 1.2 V and pH 6.[54] At lower pH values, the H^+ concentration increases and H^+ competes for adsorption sites in the aerogel pores.

Modifying AC fiber electrodes with manganese(IV) oxide (ACF/MO) increased the adsorption capacity from 2.33 mg g^{-1} for the AC fiber alone to 14.88 mg g^{-1} (Langmuir fit max) at 1.5 V.[55] It is likely that the incorporation of MO enabled Cd(II) removal *via* ion intercalation. Simulations of Cd(II) adsorption onto Mn_3O_4 (reduced from MnO_2) showed a greater energetic reward than adsorption onto graphene layers. These ACF/MO electrodes removed 65.12% of the Cd from a 200 μg L^{-1} Cd(II) solution. When the ionic strength of the 200 μg L^{-1} Cd(II) solution was raised by adding 0.1 mol L^{-1} NaCl (5.84 g L^{-1}), the Cd removal increased to 79.63%. However, raising the ionic strength again by increasing the NaCl concentration to 0.2 mol L^{-1} (11.7 g L^{-1}) decreased the removal back to 65.12%.

2.2.2 Other electrodes. Electrodes made from birnessite, a manganese oxide commonly used for supercapacitors, removed 900.7 mg Cd per g from 2200 mg L^{-1} solution at pH 6 and 0.9 *vs.* SCE.[56] While these birnessite electrodes showed

Table 2 Cadmium

Species	Electrode material	Specific surface area (m^2 g^{-1})	Voltage/charge	Initial concentration	Percent of heavy metal removed	Electrosorption capacity (mg g^{-1})	Operation time	pH	Ref.
Cd(II)	Activated carbon (AC) cloth	—	1.2 V	0.5 mM (56.2 mg L^{-1})	31.85%	—	120 min	3.8	13
		—	0.6 V	0.5 mM (56.2 mg L^{-1})	16.31%	—	120 min	3.8	
		—	0 V	0.5 mM (56.2 mg L^{-1})	4.20%	—	120 min	3.8	
		—	1.2 V	0.05 mM (5.62 mg L^{-1})	41.87%	—	120 min	—	
		—	0.6 V	0.05 mM (5.62 mg L^{-1})	21.97%	—	120 min	—	
Cd(II)	Carbon aerogel (CA)	—	1.2 V	200 mg L^{-1}	97.50%	—	40 min	6	54
		—	1.2 V	200 mg L^{-1}	81.50%	—	40 min	4	
		—	1.2 V	200 mg L^{-1}	71%	—	40 min	2	
Cd(II)	Birnessite	14.2	0.9 V *vs.* SCE	200 mg L^{-1}	—	54.78	—	3	56
		14.2	0.9 V *vs.* SCE	200 mg L^{-1}	—	196.5	—	4	
		14.2	0.9 V *vs.* SCE	2200 mg L^{-1}	—	900.7	—	6	
		14.2	0 V *vs.* SCE	2200 mg L^{-1}	—	125.8	—	6	
Cd(II)	AC fiber/MnO_2	—	1.5 V	—	—	14.88 (Langmuir fit max)	180 min	6	55
	AC fiber	—	1.5 V	—	—	2.33 (Langmuir fit max)	180 min	6	
Cd(II)	Polypyrrole/chitosan composite	—	1.5 V	1000 mg L^{-1}	51.10%	—	60 min	—	20

great uptake capacity, Mn^{2+} leached out of the birnessite during the discharge process. In the absence of Cd^{2+}, 3.40% of the Mn in the birnessite electrodes leached out and at 2200 mg L^{-1} Cd^{2+}, 38.02% of the Mn in the birnessite electrodes leached out.

Electrodes made by depositing polypyrrole on chitosan removed 51.1% of Cd from a 1000 mg L^{-1} solution at 1.5 V.[20] Polypyrrole captures Cd^{2+} through an electrochemical ion exchange mechanism. Polypyrrole typically has poor stability as an electrode so the chitosan was added to improve the stability of the polypyrrole. These polypyrrole/chitosan electrodes showed >97% regeneration through 10 charge/discharge cycles.

2.3 Chromium

Chromium is a common pollutant due to its widespread industrial use, with elevated levels of chromium in water and soil found in the US, UK, Brazil, India, Mexico, Australia, Poland, Slovenia, China, Russia, and Italy.[57,58] In water, chromium is most commonly found in the +6 and the +3 oxidation states.[59] Almost all Cr(VI) in the environment originates from human activities and Cr(VI) species are highly soluble, toxic and carcinogenic.[57] The most common Cr(VI) species are $Cr_2O_7^{2-}$, CrO_4^{2-}, $HCrO_4^-$, and H_2CrO_4. Cr(III) species are less toxic and can be precipitated out of solution as $Cr(OH)_3$.[59] Cr(III) species also include Cr^{3+}, $Cr(OH)^{2+}$, and $Cr(OH)_2^+$.[60] Cr(VI) species are generally anionic while Cr(III) species are generally cationic, so the two different oxidation states of chromium will be attracted to different electrodes.[61] Since Cr(VI) species are strong oxidizing agents, they are readily reduced to Cr(III) species:[57]

$$Cr_2O_7^{2-} + 14H^+ + 6e^- \rightarrow 2Cr^{3+} + 7H_2O$$

As a result, electrochemical removal of chromium often involves the reduction of Cr(VI) species to Cr(III) species. The pH of the solution can affect the removal of Cr in several different ways. In general, a decrease in pH is associated with a decrease in Cr(III) adsorption, an increase in Cr(VI) adsorption, and an increase in the amount of Cr(VI) reduction.[60] The WHO guideline value for Cr in drinking water is 50 μg L^{-1} and the US EPA MCL for Cr in drinking water is 100 μg L^{-1}.[34,53]

2.3.1 Activated carbon electrodes. As with arsenic and cadmium electrosorption, AC is a popular material for the chromium electrosorption of due to its high specific surface area, good conductivity, and electrochemical stability and its popularity can be seen in Table 3.[62] Different forms of plant waste have been used as carbon sources to make AC electrodes. AC derived from peach pits,[63] corncobs,[64] and Bael fruit shell[65] have been shown to be effective materials for treating Cr-containing water. Three different ACs: a commercially available AC (Loba Chemie, Mumbai, India),[66] AC prepared from tea waste biomass,[67] and AC prepared from *Limonia acidissima* (wood apple) shell[68] were used to remove Cr(VI) and F^- from 10 mg L^{-1} Cr, 10 mg L^{-1} F^- solutions. Under a potential of 1.2 V, the commercially available AC showed the highest Cr(VI) uptake and most effective removal of both Cr(VI) and F^-, removing 97.1% of Cr(VI) from the 10 mg Cr per L solution after two hours (Table 3). The AC from *L. acidissima* shells performed slightly worse, removing only 92.2% of Cr(VI) under the same conditions, and the AC from tea waste biomass had the lowest removal percentage of the three at 88.5%.

Table 3 Chromium

Species	Electrode material	Specific surface area (m^2 g^{-1})	Voltage/charge	Initial concentration	Percent of heavy metal removed	Electrosorption capacity (mg g^{-1})	Operation time	pH	Ref.
Cr(VI)	Tea waste biomass activated carbon	—	1.2 V	10 mg L^{-1}	88.50%	0.7	120 min	7.1	67
				100 mg L^{-1}	32.45%	2.83	120 min	—	
Cr(VI)	Activated carbon (AC)	—	1.2 V	10 mg L^{-1}	97.10%	0.85	120 min	7.2	66
				100 mg L^{-1}	42%	3.67	120 min	—	
Cr(VI)	*Limonia acidissima* shell AC	—	1.2 V	10 mg L^{-1}	92.20%	0.8086	120 min	7.2	68
Cr(VI)	MIL-53(Fe) and AC coated graphite	—	1.3 V	50 mg L^{-1}	39.4%	—	160 min	—	73
Cr(III)	AC cloth	—	1.2 V	0.5 mM (26 mg L^{-1})	52.48%	—	120 min	3.8	13
			0.0 V	0.5 mM (26 mg L^{-1})	41.52%				
Cr(III, VI)	Carbon aerogel (CA)	400–1100	0.9 V	35 μg L^{-1}	71% (10 ppb outlet)	—	—	7.4	69
Cr(VI)	Single wall (SW) carbon nanotubes (CNT)	380	2.5 V	6.41 mg L^{-1}	97.4%	—	240 min	4	72
Cr(VI)	CA	700 (BET)	0.8 A h	2 mg L^{-1}	99.6%	—	—	2	61
			0.8 A h	8 mg L^{-1}	96.5%	—	—	2	
Cr(VI)	Polyvinylferrocene	—	0.8 V *vs.* Ag/AgCl	1 mM (52 mg L^{-1})	—	~100	—	5	40
			0.8 V *vs.* Ag/AgCl	100 μg L^{-1}	>80%	—	4 h		
Cr(III, VI)	CNT	36.6 (BET)	−1.4 V *vs.* SHE	12 mg L^{-1}	96%	—	115 min	3	71
Cr(VI)	Porous carbon (Corncob Biomass)	952	2 V	30 mg L^{-1}	96.20%	—	160 min	—	74
Cr(VI)	AC fibre felt	1104.52	1.2 V	20 mg L^{-1}	—	11.6	10 h	6	62
			1.2 V	300 mg L^{-1}	—	84	20 h	—	
Cr	AC (Peach Stones)	623	−1.4 V *vs.* SCE	236.62 mg L^{-1}	96%	—	11 h	—	63

Activated carbon cloth (ACC, FM70) removed 52.48% of the Cr^{3+} from a 0.5 mM Cr^{3+} (26 mg L^{-1}) solution at 1.2 V.[13] This Cr^{3+} removal rate was the higher than the removal rates for Cd^{2+} and Pb^{2+} under the same conditions (0.5 mM Cd^{2+} (56.2 mg L^{-1}) or Pb^{2+} (104 mg L^{-1})), likely because Cr^{3+} has a greater charge than the other two ions. In a competitive heavy metal removal test, 0.5 mM Pb^{2+} and 0.5 mM Cd^{2+} were added to the 0.5 mM Cr^{3+} solution and the ability of the electrode to remove Cr^{3+} decreased only slightly in the presence of Cd^{2+} and Pb^{2+} as the removal efficiency decreased from 52.48% to 46.22%.

Treatment of AC fiber felt with nitric acid increased the felt surface area, and the resulting material could adsorb 17.75 mg g^{-1}, whereas the untreated AC fiber felt could only adsorb 11.47 mg g^{-1}.[62]

2.3.2 Other carbon and composite electrodes. Other forms of carbon such as aerogels and nanotubes have been used as electrodematerials for the treatment of chromium contaminated water. Carbon aerogel electrodes have lower resistivity than activated carbon electrodes, and do not require polymers binders that may degrade over time or obstruct adsorbent sites.[69] However, a large portion of their surface area is inaccessible, their pore dimensions are often of similar size as the thickness of the double layer, resulting in electrical double layer overlap.[70] Carbon aerogels were used to selectively lower the Cr concentration in groundwater from 30–35 ppb to 8 ppb with the application of a 1.2 V potential.[69] Two carbon aerogels with 0.8 A h charge placed between could achieve greater than 99% removal of Cr from a 2 mg L^{-1} solution at a pH of 2.[61] These same carbon aerogels also showed greater than 90% removal in experiments with 8 mg L^{-1} chromium with only 0.3 A h charge (Table 3). However, the performance of these electrodes dramatically decreased at more alkaline pH values as species such as $Cr(OH)_3$ began to form. At constant concentration 8 mg L^{-1} and charge 0.8 A h, 75% of the Cr was removed at pH 7, compared to 96.5% at pH 2.

Electrodes made of vertically aligned CNTs grown on stainless steel mesh were shown to be able to adsorb and reduce Cr(VI) simultaneously.[71] These CNT electrodes could reduce 96% of the Cr(VI) in a 12 mg L^{-1} solution at a potential of −1.4 V in 115 minutes and adsorbed 746 mg m^{-2}. Single-wall CNT coated stainless steel net electrodes (SWCNTs@SSN) also removed Cr(VI) by simultaneous reduction and adsorption.[72] At a potential difference of 1 V, the SWCNTs@SSN electrodes only removed 6.5% of the total chromium. However, at a potential difference of 2.5 V, 97.4% of the total chromium was removed.

Across the tested range of pH 2–5, total chromium removal was maximized at pH 4. At higher pH, Cr(VI) was less likely to be reduced to Cr(III) and at lower pH, Cr(III) can form a large hydrated complex $Cr(H_2O)_6^{3+}$ which may block further chromiumfrom being adsorbed.

2.3.3 Synergetic capture of Cr(VI) and conversion to Cr(III). As presented in the previous studies, reduction of Cr(VI) to Cr(III) often occurs concurrently with Cr electrosorption. This section highlights Cr electrosorption processes that have components specifically designed to reduce Cr(VI) to Cr(III), both using redox-active platforms as well as activated carbon.

Redox-active systems are attractive for selective separation and conversion due to their chemical tunability,[75] reversibility of the electron-transfer process, electrocatalytic properties,[76] and associated energy storage capabilities.[77–79] Ferrocene-containing systems in particular can be heterogeneously immobilized onto conductive films, presenting electroresponsive properties in the heterogeneous form.[77,80] Films containing redox-active polymer poly(vinyl)ferrocene (PVF) and CNTs were used as an adsorbent to remove Cr and As species from water.[40] This PVF–CNT composite showed a maximum uptake above 100 mg g^{-1} Cr at 0.8 V *vs.* Ag/AgCl from a 1 mM Cr (52 mg L^{-1}) solution. The application of a positive potential oxidized the PVF ferrocene units into ferrocenium, which then formed ion pairs with the Cr(VI) species. PVF selectively adsorbed Cr(VI) and As(V) oxyanions in the presence of ClO_4^- or Cl^-. This selectivity was largely dictated by charge transfer interactions between the positive ferrocenium and negative anions. Since ClO_4^- and Cl^- are more electronegative and less polarizable than the Cr(VI) species, ClO_4^- and Cl^- transferred less charge to the oxidized PVF and bonded weakly. Upon applying a reducing potential, Cr(VI) was converted to the less toxic Cr(III) and desorbed from the electrode (Fig. 2).

A photocatalysis-CDI system (PCS) reduced Cr(VI) to Cr(III) while removing it from solution using CDI.[73] The positive electrode was made of photocatalyst MIL-53(Fe), and the negative electrode was made of AC. Upon exposure to light, anionic Cr(VI) species embedded in the MIF-53(Fe) electrode were reduced to Cr(III), which are cationic. These Cr(III) cations then migrated to and adsorbed onto the AC electrode, allowing both electrodes to participate in electrosorption. This system could achieve up to 81.6% removal of Cr(VI) from a 50 ppm solution with an applied voltage of 1.3 V after 160 minutes, higher than the removal percentage achieved by photocatalysis or by AC adsorption alone (Fig. 3).

2.4 Copper

Copper is a common heavy metal pollutant released from industrial processes such as circuit printing and metal plating and from corroding copper plumbing.[81,82] Copper concentrations in drinking water vary widely as Cu levels in running and fully flushed water are usually lower, while Cu

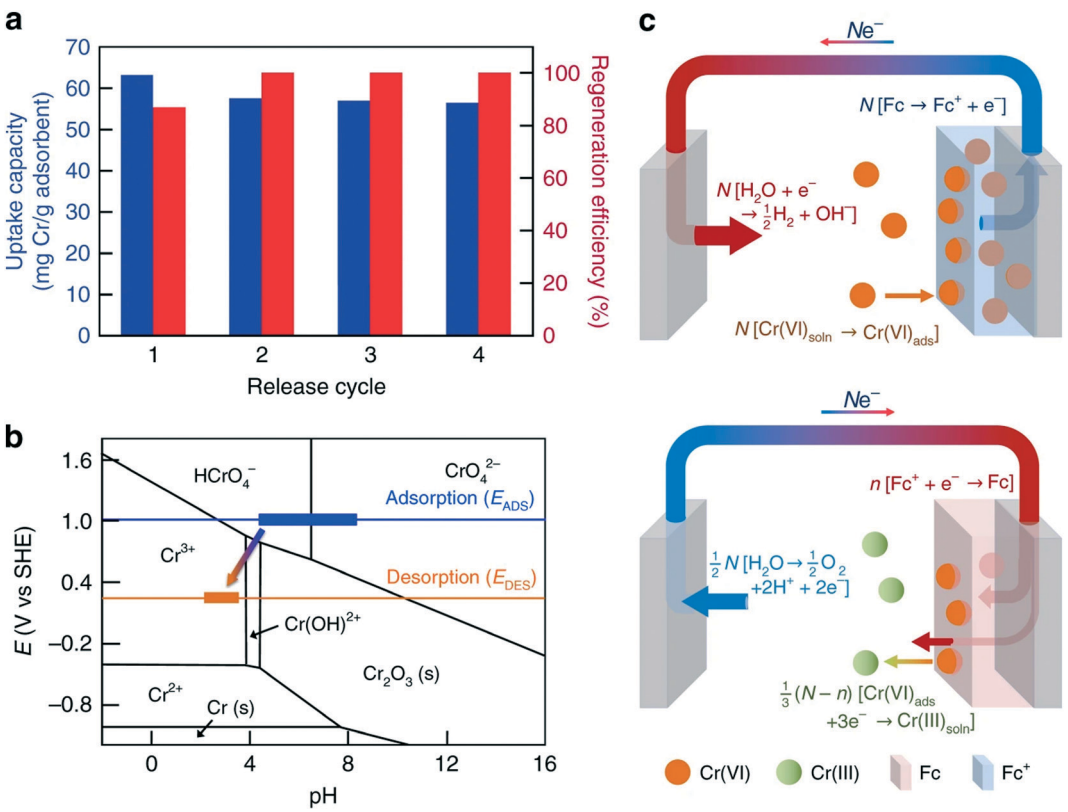

Fig. 2 Selective capture-and-release of Cr using polyvinylferrocene coated electrodes. These electrodes captured Cr(VI) and converted Cr(VI) to a less toxic Cr(III) upon release. (a) These electrodes showed great stability and recyclability over several discharge cycles; complete recovery of Cr was obtained for every cycle after the first. (b) The *E*-pH diagram for Cr speciation showing the conditions at which adsorption and desorption occurred. (c) Schematic of the faradaic reactions that occur at each electrode during adsorption and desorption. Reproduced from ref. 40 with permission from Springer Nature, copyright 2019.

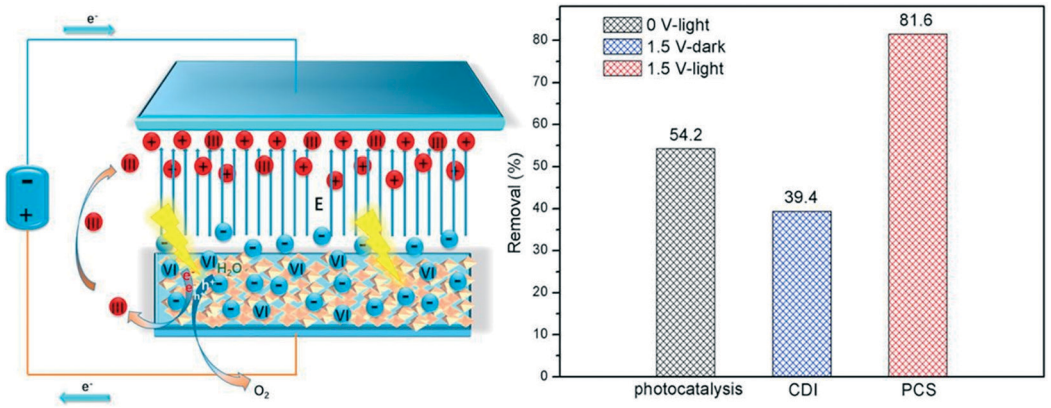

Fig. 3 Synergistic conversion and removal of Cr by a photocatalysis and capacitive deionization system (PCS). Cr(VI) species are anionic and only attracted to the anode in a CDI system. By photocatalytically reducing Cr(VI) to Cr(III), which are typically cationic species, both the cathode and anode could be utilized to capture Cr. Reproduced from ref. 73 with permission from Elsevier, copyright 2019.

levels in standing or partially flushed water can be much higher.[82] Elevated levels of copper contamination in drinking water have been recorded in various locations across the US, Canada, Sweden, and Germany.[82] Although acute toxicity requires very high levels of copper, individuals with genetic disorders such as Wilson's disease can suffer from the accumulation of copper in their brain, kidneys, and liver. In some cases, high levels of copper can cause liver damage.[83] The WHO guideline value for copper in drinking water is 2 mg L^{-1} and the US EPA action level for copper is 1.3 mg L^{-1}.[34,53]

Copper is one of the most commonly studied heavy metals in electrosorptive processes. Generally, Cu removal through electrosorption or CDI is most effective in slightly acidic solutions. Table 4 lists the best electrosorptive performances reported by various studies and most of them occur at pH 4 or 5. In more acidic solutions, there is more competition between Cu^{2+} and H^+ for adsorption sites, and in alkaline solutions, copper can form an insoluble hydroxide compound.[84–86] In some cases, the reduction and deposition of Cu metal can impact the performance of electrosorptive or CDI systems.[87–89]

2.4.1 Activated carbon electrodes. ACs from a wide variety of sources have been used as electrode material for Cu removal. Commercially available AC (Filtrasorb 400, Chemviron Carbon Inc.) had a maximum uptake of 24.57 mg g^{-1} under a potential of 0.8 V, showed good regenerative ability, and remained effective in the presence of natural organic matter (NOM) and NaCl.[90] The removal capacity of this Filtrasorb 400 AC electrode from a 50 mg L^{-1} Cu solution changed from 2.48 to 2.39 to 2.21 mg g^{-1} as the NaCl concentration increased from 0.001 to 0.01 to 0.1 M. A different AC electrode (named AG-3V) reached uptakes up to approximately 30 mg g^{-1} from 500 mg L^{-1} at 0 V *vs.* Ag/AgCl.[91]

Polyacrylonitrile-based AC fiber cloths modified with either a chitosan solution or by a nitric acid wash showed increased removal capacity after modification.[81] Although these treatments resulted in a lower surface area, the HNO_3 and chitosan modifications improved uptake from 24.7 mg g^{-1} (unmodified) to 32.8 mg g^{-1} (nitric acid) and 54.3 mg g^{-1} (chitosan). Increased uptake was attributed to the increase of functional groups (carboxyl groups for the nitric acid treated AC and the increase in hydroxyl and amine groups for the chitosan modified AC) that promote binding to heavy metals.

2.4.2 Other carbon electrodes. Carbon aerogels can also be used to specifically adsorb Cu^{2+} ions.[92] Carbon aerogels can be synthesized by stirring together resorcinol and formaldehyde in the presence of a sodium carbonate solution as a catalyst.[93] The resorcinol to catalyst (*R*/*C*) ratio of carbon aerogels synthesized in this manner impacts their surface properties and their adsorption capacities. Aerogels made with five different *R*/*C* ratios between 330 and 1530 showed Cu^{2+} capacities ranging from 29.7 mg g^{-1} for 1030 *R*/*C* to below 10 mg g^{-1} for 830 *R*/*C* in a 100 mg L^{-1} $CuSO_4$ solution and under a potential of 1.2 V. A more comprehensive list is given in Table 4.

Modification of aerogel electrodes, such as combining aerogels with other materials to make composite electrodes or doping aerogels with heteroatoms, can improve the capacity of aerogel electrodes. Under a 1.2 V potential, unmodified carbonaceous aerogels had a capacity of 30.35 mg g^{-1}, while aerogels modified with Fe_2O_3, CeO_2, and TiO_2 had capacities from about 41.42, 49.28, and 57.13 mg g^{-1}, respectively.[94] The aerogels modified with TiO_2 also showed excellent stability, retaining 96% of their capacity after 1000 adsorption–desorption cycles. The uptake of Cu^{2+} onto 3D graphene aerogel could be controlled by sulfur and/or nitrogen heteroatom doping.[95] S-Doped aerogels had a maximum capacity of 166.5 mg g^{-1} and were more effective than the N-doped gels or the S,N-codoped gels which had capacities of 119.9 mg g^{-1} and124.4 mg g^{-1}, respectively. This is consistent with hard–soft-acid–base theory. Since S is softer than N, the S-doped aerogels should therefore interact more favorably with soft heavy metal ions.

Table 4 Copper

Species	Electrode material	Specific surface area ($m^2\ g^{-1}$)	Voltage/charge	Initial concentration	Percent of heavy metal removed	Electrosorption capacity (mg g^{-1})	Operation time	pH	Ref.
Cu(II)	Reduced graphene oxide–titanium dioxide nanotubes	511.226	1.2 V	80 mg L^{-1}	—	253.25	120 min	—	102
Cu(II)	Fe_3O_4–Graphene nanocomposite	—	1.2 V	0.3 mM (19.1 mg L^{-1})	~80%	—	—	6.1–7.1	100
			1.2 V	0.03 mM (1.91 mg L^{-1})	~85%	—	—	6.1–7.1	
Cu(II)	Carbon aerogel (CA) resorcinol/catalyst (*R*/*C*) = 300	832	1.2 V	100 mg L^{-1}	~55%	~20	—	—	93
	CA *R*/*C* = 500	2177	1.2 V	100 mg L^{-1}	~75%	~14			
	CA *R*/*C* = 800	1496	1.2 V	100 mg L^{-1}	~40%	~7			
	CA *R*/*C* = 1000	2057	1.2 V	100 mg L^{-1}	~75%	29.7			
	CA *R*/*C* = 1000	2057	1.5 V	100 mg L^{-1}	85.4%	25.78			
	CA *R*/*C* = 1500	2188	1.2 V	100 mg L^{-1}	~60%	12			
Cu(II)	Carbon nanotubes (CNT) – nanofibers (CNF)	121.22	1.4 V	151.1 μg L^{-1}	90.7%	0.137	—	—	97
Cu(II)	MnO_2–Carbon fiber	−0.8 V	—	6 mg L^{-1}	—	145.42	24 h	5	85
Cu(II)	Ordered mesoporous carbon (OMC)	1410	0.9 V	200 mg L^{-1}	—	56.62	—	4	84
Cu(II)	OMC	487	0.8 V	50 mg L^{-1}	—	44.48	5 h	5	96
Cu(II)	Activated carbon fiber (ACF) cloth	1294.3	0.3 V	100 mg L^{-1}	—	0.386 mmol g^{-1} (24.5 mg g^{-1})	12 h	4	81
	ACF-modified w/ nitric acid	1209.3	0.3 V	100 mg L^{-1}	—	0.482 mmol g^{-1} (30.6 mg g^{-1})	12 h	4	
	ACF-chitosan	1123.3	0.3 V	100 mg L^{-1}	—	0.969 mmol g^{-1} (61.6 mg g^{-1})	12 h	4	
Cu(II)	AC	964 (BET)	0.8 V	50 mg L^{-1}	—	2.48	200 min	5	90
Cu(II)	Zn–S decorated active carbon felt (ACF)	29.75 (BET)	−0.2 V	100 mg L^{-1}	—	27.4	100 min	5	86
	FeS–ACF	12.5 (BET)	−0.2 V	100 mg L^{-1}	—	18	100 min	5	
	ACF	11.9 (BET)	−0.2 V	100 mg L^{-1}	—	12.2	100 min	5	
Cu(II)	Poly(*m*-phenylenediamine) paper (P*m*PD)	—	−0.3 V *vs.* SCE	3 mmol L^{-1} (190 mg L^{-1})	—	123	—	—	104
Cu(II)	CA	—	1.2 V	200 mg L^{-1}	—	30.353	—	5	94
	CA–TiO_2	282.1 (BET)	1.2 V	200 mg L^{-1}	—	57.134	—	5	
	CA–CeO_2	222.7 (BET)	1.2 V	200 mg L^{-1}	—	49.281	—	5	
	CA–Fe_3O_4	262.6 (BET)	1.2 V	200 mg L^{-1}	—	41.424	—	5	
Cu(II)	P*m*PD/reduced graphene oxide	—	−0.3 V *vs.* SCE	5 mM (318 mg L^{-1})		376.8	—	—	105
			−0.3 V *vs.* SCE	0.25 mM (15.9 mg L^{-1})	80.3%	—	2 min	—	
Cu(II)	AC cloth	1000	1.2 V	7.5 mM (477 mg L^{-1})	62%	—	3 hours	—	88
Cu(II)	Crumpled N-doped graphene nanosheets	695	1.2 V	200 ppm (200 mg L^{-1})	~100%	498	30 min	—	99
Cu(II)	Chitosan–sodium phytate/polyethylene glycol terephthalate	8.9	1.2 V	10 mg L^{-1}	88%	8.96	7 h	—	107
Cu(II)	AC fiber	1384.2	1.2 V	500 mg L^{-1}	—	108.7	—	—	87
Cu(II)	S-Doped 3D graphene aerogels (3DGA)	481	−0.3 V *vs.* SCE	—	—	166.5 max	1 min	N/A	95
	N-Doped 3DGA	434	−0.3 V *vs.* SCE	—	—	119.9 max			
	S,N-Codoped 3DGA	443	−0.3 V *vs.* SCE	—	—	124.4 max			
Cu(II)	Birnessite	75	0.4–0.9 V *vs.* SCE	2200 mg L^{-1}	—	372.3	—	—	103
			0.4–0.9 V *vs.* SCE	200 mg L^{-1}	—	115	—	—	
			0.0–0.9 V *vs.* SCE	200 mg L^{-1}	—	236.4	—	—	
Cu(II)	Carbon aerogel	412	1.2 V	~75 mg L^{-1}	—	~1.1	4 h	—	92
Cu(II)	CNT–CNF composite films	—	2 V	50 μS cm^{-1} $CuCl_2$	>90%	N/A	60 min	—	98

Table 4 *(continued)*

Species	Electrode material	Specific surface area ($m^2\ g^{-1}$)	Voltage/charge	Initial concentration	Percent of heavy metal removed	Electrosorption capacity ($mg\ g^{-1}$)	Operation time	pH	Ref.
Cu(II)	Polypyrrole/chitosan/CNT composite	33.51	0.8 V	250 mg L^{-1}	47.42%	23.8	30 min	—	106
Cu(II)	Polypyrrole/chitosan	—	1.5 V	1000 mg L^{-1}	49.83%	99.67	60 min	—	20

The removal ratio for Cu^{2+} was higher than the ratio for Pb^{2+}, Hg^{2+}, and Cd^{2+} in these S/N doped aerogels, possibly because Cu^{2+} has the smallest hydrated radius.

Ordered mesoporous carbon (OMC) electrodes were able to adsorb 56.62 mg Cu/g from a 200 mg L^{-1} Cu solution under a potential of 0.9 V, substantially more than electrodes made of a commercially available AC (AW ACF) (16.02 mg g^{-1}) under the same conditions.[84] While the AW ACF electrodes had a much higher specific surface area (1294 $m^2\ g^{-1}$) than the OMC electrodes (487 $m^2\ g^{-1}$), most of the surface area of the AW ACF electrodes was formed by micropores, which were too small for the Cu^{2+} ions to access. The addition of a chelating agent, such as citric acid or ethylenediaminetetraacetic acid (EDTA), to Cu containing solutions can increase the electrosorption capacity of ordered mesoporous carbon.[96] While free Cu^{2+} is generally adsorbed to the cathode, Cu–EDTA complexes are negatively charged and are attracted to the anode. In the absence of chelating agent, OMC electrodes removed 35.9 mg g^{-1} Cu from 50 mg L^{-1} solution at pH 4. The addition of a chelating agent in a 10/1 Cu/chelating agent ratio increased the adsorption capacity to 70.18 mg g^{-1} for citric acid and 59.26 mg g^{-1} for EDTA.

CNTs and carbon nanofibers (CNFs) are commonly used electrode materials for Cu electrosorption due to their high specific surface areas and good electrical conductivity.[97,98] CNT–CNF films used to electrosorb Fe^{3+}, Cu^{2+}, Zn^{2+}, and Na^{+} had ion electrosorption capacities in the order of $Fe^{3+} > Cu^{2+} > Zn^{2+} > Na^{+}$.[70] This order can be explained by the charge and hydrated radii of the ions. Ions with higher charge were more easily adsorbed onto the electrode under the effect of an electric field. For ions with the same charge, the size of their hydrated radius dictates adsorption behavior. Ions with a smaller hydrated radius adsorb more easily and, in this case, the hydrated radius of Cu^{2+} is smaller than that of Zn^{2+} so Cu^{2+} is preferentially adsorbed compared to Zn^{2+}. Electrosorption tests on N-doped graphene nanosheets showed a similar trend, with the electrosorption rate of Fe and Cu ranking first and second among 9 different metal ions.[99] Cu adsorbed quickly onto the N-doped graphene nanosheets because Cu^{2+} has a strong affinity to complex with hydroxyl groups on the surface of the graphene nanosheets.

2.4.3 Metal-oxide and metal-sulfide composite electrodes. Modifying carbon electrodes with metal-oxide and metal-sulfide materials to make composite electrodes can improve their Cu uptake capacity. A Fe_3O_4/porous graphene nanocomposite was able to remove more Cu^{2+} from 0.03 mM Cu^{2+} (1.91 mg L^{-1}) solution than pure porous graphene from 0.03 mM Cu^{2+}, and these graphene electrodes also removed Pb^{2+} and Cd^{2+} at efficiencies very similar to their Cu^{2+} removal efficienies.[100] Porous graphitic carbon nanosheets from sugarcane bagasse functionalized with Fe_3O_4 nanoparticles removed more than 90% of every heavy metal ion from a mixture of 0.5 mg L^{-1} Mg^{2+}, Zn^{2+}, Cu^{2+}, Cd^{2+} and Pb^{2+} each.[101] A composite material containing reduced graphene oxide and TiO_2 nanotubes (rGO–TNT) could achieve a Cu^{2+} uptake of 253.25 mg g^{-1} from an 80 mg L^{-1} Cu^{2+} solution under a potential of 1.2 V.[102] On a molar basis, the rGO–TNT electrodes showed a strong preference for Cu^{2+} (3.99 mmol g^{-1} or 253.5 mg g^{-1}) over Pb^{2+} (1.17 mmol g^{-1} or 242.4 mg g^{-1}), possibly due to the smaller size and higher reduction potential of Cu^{2+} ions. The addition of ZnS improved the adsorptive capacity of carbon felt electrode more than FeS.[86] The addition of FeS or ZnS to active carbon felt (ACF) electrodes improved Cu^{2+} adsorption from 12 mg g^{-1} (ACF) to 18 mg g^{-1} (ACF–FeS) or 27.4 mg g^{-1} (ACF–ZnS) from 100 mg L^{-1} Cu^{2+} solution at −0.2 V. Adding 150 mg L^{-1} Cr^{3+} only decreased the ACF–ZnS Cu^{2+} electrosorption capacity from 27.4 mg g^{-1} to 23.5 mg g^{-1}.

A MnO_2/carbon fiber composite electrode had a maximum adsorption capacity of 172.88 mg g^{-1} under a potential of 0.8 V.[85] Birnessite, a redox active manganese oxide-based mineral, has showed an electrosorption capacity of 372.3 mg g^{-1} after 30 charge–discharge cycles between 0.4–0.9 V *vs.* SCE.[103] These electrodes captured Cu^{2+} by intercalating cations when the Mn(IV) in birnessite was reduced to Mn(III). The adsorption capacity of the birnessite electrodes increased after each charge–discharge cycle because Cu^{2+} formed stable inner-sphere complexes with birnessite. As a result, Cu^{2+} was not completely desorbed during the oxidation of birnessite and accumulated with each cycle.

2.4.4 Polymer electrodes. Several different organic polymers have been investigated for their ability to remove Cu^{2+}. A poly(*m*-phenylenediamine) (P*m*PD) electrode was found to have an uptake of 123 mg g^{-1} in a 3 mM Cu^{2+} (191 mg L^{-1}) solution.[104] The optimal voltage for Cu^{2+} removal was −0.3 V *vs.* SCE as decreasing the potential below −0.3 V *vs.* SCE reduced water and showed bubbles on the surface of the P*m*PD electrode. The negative potential not only increased the electrostatic attraction between the Cu^{2+} ions and the P*m*PD electrode, it also increased the presence of imine structures in the polymer that chelate Cu^{2+}. Electrodes

made of P*m*PD on reduced graphene oxide exhibited similar behavior had a 376.8 mg g^{-1} capacity at a 5 mM Cu^{2+} (318 mg L^{-1}) concentration and −0.3 V *vs.* SCE.[105] The reduced graphene oxide provided conductivity and mechanical strength that improved the efficiency and regeneration ability of P*m*PD.

A composite electrode made from chitosan and polypyrrole, a conductive polymer, showed Cu^{2+} uptakes as high as 99.67 mg g^{-1}, and it removed other metal ions such as Ag^{+}, Pb^{2+}, and Cd^{2+} at rates similar to its Cu^{2+} removal rate.[20] An electrode containing polypyrrole, chitosan, and CNTs showed Cu^{2+} uptakes of up to 19.2 mg g^{-1}, which was slightly less than its capacity for Fe^{3+} (22.3 mg g^{-1}) but more than its capacity for Ag^{+} (17.9 mg g^{-1}).[106] An electrode made from chitosan and sodium phytate supported on polyethylene glycol terephthalate could remove 88% of Cu^{2+} from a 10 mg L^{-1} stream when a potential of 1.2 V was applied.[107]

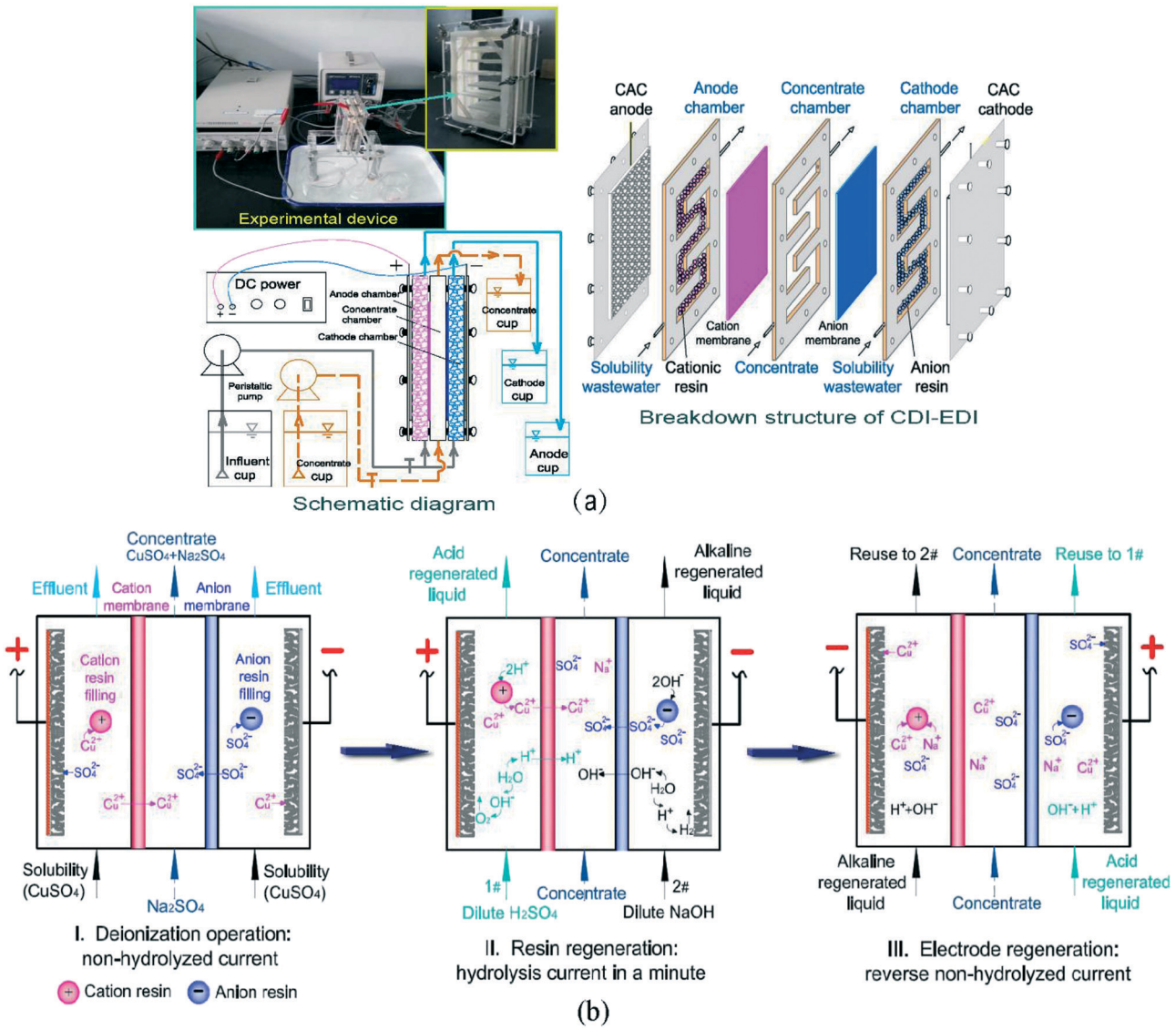

Fig. 4 (a) Schematics of a combined CDI–electrodeionization (EDI) water remediation apparatus. This CDI–EDI system purifies wastewater through a combination of electrosorption and ion exchange. For this system, the wastewater stream of $CuSO_4$ is fed into the anode and cathode chambers and a concentrate salt solution of Na_2SO_4 is fed into the middle chamber. The cathode and anode chambers are filled with their corresponding resins to further increase the chamber's affinity for ions of a specific charge. The first step is to pass the feed through the apparatus with <4.0 mA so Cu(II) in the anode chamber is removed from solution in a 3-step process. (b) In step one, the feed stream is passed into each of the electrode chambers. In the anode chamber, Cu(II) can either bind to the cation exchange resin or pass through the cation membrane into the salt concentrate chamber. In the cathode chamber, the Cu(II) ions can undergo electrosorption. The second step involves resin regeneration with acid and base generated by hydrolysis. In this study, the current was raised above 4.0 mA to generate protons in the anode chamber that could regenerate the cation resin so the Cu(II) can flow into the concentrate chamber. In the cathode chamber, hydroxide ions can displace the SO_4^{2-} into the concentrate. The final step is to regenerate the electrodes by reversing the potential across the electrodes. While the potential is reversed, the effluents from the anode and cathode chambers are recycled into the opposite chamber to remove the remaining ions. This technology was able to achieve a 95.7% and 87.6% removal efficiency for the anode and cathode chambers, respectively, with a starting Cu(II) concentration of 42.9 mg L^{-1} and a specific surface area of 2100 m^2 g^{-1}. Reproduced from ref. 26 with permission from Elsevier, copyright 2019.

2.4.5 Membrane-augmented CDI. Membrane CDI with AC fiber electrodes was used to remove Cu^{2+} and Zn^{2+} from water, and the adsorption capacity at 1.2 V in a 500 mg L^{-1} solution was found to be 108.7 mg g^{-1} for Cu^{2+} and 122.6 mg g^{-1} for Zn^{2+}.[87] At voltages from 0.4 to 0.6 V, Cu^{2+} adsorption capacities were greater than adsorption capacities of Zn^{2+}, possibly due to the smaller hydrated radius of Cu^{2+}. At voltages between 0.8–1.2 V, the amount of Zn^{2+} adsorbed was greater than that of Cu^{2+}, likely because at voltages above 0.6 V, Cu^{2+} reduced and deposited on the electrode as Cu and Cu_2O, which decreased the surface area of the electrode.

A novel CDI–electrodeionization process combining ion-exchange membranes and resins was able to remove 95.7% of the copper from a 42.9 mg L^{-1} solution.[26] This system involved three chambers separated by ion-exchange membranes: an anode chamber, a cathode chamber, and a concentrated chamber located between them. $CuSO_4$ was adsorbed onto AC electrodes in the anode and cathode chambers while being enriched in the concentrated chamber, making it a useful technology for both water purification and resource recovery (Fig. 4).

2.5 Iron

Iron poisoning typically occurs due to the accidental ingestion of large doses of iron, and it can lead to vomiting, diarrhea, and liver damage.[83] Iron in ground water originates from iron-containing rock and it is common to find iron in ground water in many geographical areas around the globe because iron is very abundant; iron makes up about 5% of the Earth's crust.[108] Comparatively little research has been done on the removal of iron from solutions through electrosorption or CDI (Table 5).

2.5.1 Carbon electrodes. Graphene nano-flakes were used to remove $FeCl_3$ from water through electrosorption and had a maximum electrosorptive capacity of 0.88 mg g^{-1} at an applied potential of 2.0 V.[109] Because Fe^{3+} is more highly charged than many other cationic species, it is generally easier to remove by electrosorptive processes so despite having the largest hydrated radius, the graphene nanoflakes removed Fe^{3+} faster than Ca^{2+}, Mg^{2+}, and Na^{+}. A CNTs–CNFs composite film electrode could remove Fe^{3+} more rapidly than Cu^{2+}, Zn^{2+}, and Na^{+}, again, because Fe^{3+} is more charged than the other ions.[70] Fe^{2+} had the fastest removal rate onto N-doped graphene nanosheet electrodes despite the presence of many other metal cations with a 2+ charge.[99] This was likely because Fe^{2+} was oxidized to Fe^{3+}. Fe^{3+} could out-compete the other ions for adsorption sites because of its higher charge and greater affinity for hydroxyl groups on the electrode surface.

2.6 Nickel

Nickel is a potential carcinogen and can cause other health problems such as gastrointestinal distress and pulmonary fibrosis.[3,111] Reports of high nickel concentration in water typically arise from nickel leaching out of stainless steel plumbing.[113] The WHO guideline value for nickel in drinking water is 70 μg L^{-1}.[34] Various nickel electrosorption results are reported in Table 6.

2.6.1 Carbon-based electrodes. Multi-walled CNTs were used to remove Ni^{2+} had maximum uptake of 145.73 mg g^{-1}.[110] The CNTs performed better in more alkaline solutions since Ni^{2+} had less competition from H^{+} for adsorption sites. Nanoneedle-structured α-MnO_2/carbon fiber paper composite (MnO_2/CFP) electrodes were synthesized and showed an uptake of 16.4 mg g^{-1} Ni^{2+} upon the application of a −1.3 V potential.[111] This uptake was much higher than the uptake of carbon fiber paper alone (0.034 mg g^{-1}) under the same conditions. However, during nickel removal, Mn^{2+} ions were released by partial reduction of MnO_2. An asymmetric electrode cell, consisting of a MnO_2/CFP positive electrode and an AC negative electrode, was used to remove the leached Mn^{2+}, and could decrease the Mn^{2+} concentration from 100 ppm to less than 2 ppm.

2.6.2 Other electrodes. Birnessite, a mineral containing MnO_2, was combined with CNTs to make HB/CNT electrodes with increased specific area and conductivity.[112] The composite could adsorb 155.6 mg Ni^{2+} per g after 12 hours under a potential of 0 V *vs.* SCE. This adsorption capacity was higher than that of the birnessite alone (96.6 mg g^{-1}) or CNTs alone (~0 mg g^{-1}). Electrosorption was induced by reduction of manganese in the electrode from Mn(IV) to Mn(III) and Mn(II) and this reduction is accompanied the insertion of Ni^{2+} or Zn^{2+} into the electrode.

2.7 Lead

Lead is used in many processing industries such as ammunition, battery, paint, alloy, and glass making

Table 5 Iron

Species	Electrode material	Specific surface area (m^2 g^{-1})	Voltage/charge	Initial concentration	Percent of heavy metal removed	Electrosorption capacity (mg g^{-1})	Operation time	pH	Ref.
Fe(III)	Carbon nanotubes–carbon nanofibres composite film	—	1.2 V	1.5 mM (83.8 mg L^{-1})	~25%	—	—	—	70
Fe(III)	Graphene nano-flakes	254	0.8 V 2 V	20 mg L^{-1} $FeCl_3$	—	0.2 0.49	30	—	109
Fe(II)	Crumpled N-doped graphene nanosheets	695	1.2 V	10 ppm (10 mg L^{-1})	>90%	—	15 min	—	99

Table 6 Nickel

Species	Electrode material	Specific surface area (m^2 g^{-1})	Voltage/charge	Initial concentration	Percent of heavy metal removed	Electrosorption capacity (mg g^{-1})	Operation time	pH	Ref.
Ni(II)	Multi-walled CNTs	—	1.6 V	50 mg L^{-1}	—	145.73 max	60 min	—	110
Ni(II)	Nanostructured alpha-MnO_2/carbon paper composite	42.3	−1.3 V	100 ppm (100 mg L^{-1})	88.90%	16.4	120 min	—	111
	Activated carbon (AC)	633	−1.3 V	100 ppm	30.20%	2.2	120 min	—	
Ni(II)	Birnessite/CNT nanocomposites (45.6% MnO_2)	143	0 V *vs.* SCE	50 mg L^{-1}	N/A	155.6	12 h		112

operations. Large amounts of lead have been discharged in into the environment as a result of poorly controlled industrial activity.[114] Exposure to lead is especially common in low and middle-income countries.[115] Marginalized populations in places such as La Oroya, Peru[116] and Torreon, Mexico[117] are more likely to live close to toxic waste sites. Consumption of lead contaminated water can cause damage to liver, kidney, brain and nervous system.[13] Due to its high toxicity and tendency to bioaccumulate, lead was listed by the US Environmental Protection Agency as one of the priority pollutants.[118] The WHO guideline value for lead in drinking water is 10 μg L^{-1} and the US EPA action level for lead in drinking water is 15 μg L^{-1}.[34,53]

2.7.1 Activated carbon electrodes. AC can be obtained easily from a wide range of raw materials through thermal or chemical activations.[119] AC obtained from date stones achieved an adsorption capacity of 17.71 mg g^{-1} and desorption capacity of 17.02 mg g^{-1} from a 5 mg L^{-1} Pb at 0.13 V *vs.* SCE.[120] When a negative potential is applied, the electrode reduces water into hydrogen gas and hydroxyl ions. This increases the pH of the solution at the electrode surface and enables Pb^{2+} ions bind to hydroxyl and carboxylic acid groups by reactions such as:[120,121]

$$R - COOH + OH^- \rightarrow R - COO^- + H_2O$$

$$2R - COO^- + Pb^{2+} \rightarrow (R - COO^-)_2Pb^{2+}$$

When reversing the applied potential, the AC acts as the anode and oxidizes water, decreasing the pH at the electrode. The reaction will be reversed, and the electrode can be regenerated:

$$2H_2O \rightarrow 4H^+ + O_2 + 4e^-$$

$$(R - COO^-)_2Pb^{2+} + 2H^+ \rightarrow 2R - COOH + Pb^{2+}$$

2.7.2 Other carbon electrodes. Graphene is another carbon-based material that is effectively used for electrosorption because it has a large theoretical specific surface area, 2630 m^2 g^{-1}, and has higher conductivity than other carbon materials.[122] However, the graphene lamellae tend to agglomerate due to the strong π–π interaction between graphene sheets.[123] This agglomeration greatly reduces the specific surface area and conductivity of graphene. A three-dimensional framework was developed from graphene sheets with an interconnected hierarchical porous structure to overcome these limitations and enhance the ability of graphene to uptake lead .[124] Under an applied voltage of 1.4 V and pH 6, a 3DG electrode grafted with ethylenediamine triacetic acid (EDTA) achieved a high Pb^{2+} removal efficiency of 99.9% from a 140 mg L^{-1} Pb and desorbed 94.3% of the Pb after 8 cycles. The addition of EDTA to the electrode enables Pb^{2+} ions to be captured through a chelation reaction, which provided another driving force in addition to the electrostatic attraction of Pb^{2+} to the electrode. Graphene's selectivity for Pb^{2+} could be controlled with nitrogen doping.[125] Graphene doped with softer pyrrolic-N showed a greater affinity toward soft Pb^{2+} ions than graphene doped with harder pyridinic-N (Fig. 5). The performance of electrodes made with these N-doped graphenes is listed in Table 7.

Graphene sheets can also be rolled up to produce carbon nanotubes (CNTs), and the hollow layered structure of CNTs makes them a good electrode material in capacitive deionization.[126] CNT electrodes oxidized with nitric acid achieved a Pb^{2+} adsorption capacity of 15.6 mg g^{-1}.[126] The electrosorption performance of CNTs can be enhanced greatly when combined with other materials in composite electrodes. A single walled-CNT coated stainless steel net (SSN) electrode achieved Pb^{2+} removal efficiencies ranging from 97.2% to 99.6% from aqueous solutions with Pb^{2+} concentration varied between 20 mg L^{-1} to 150 mg L^{-1} after 90 minutes under an applied potential of −2.0 V *vs.* SCE.[114] Activating CNT electrodes by air-plasma to produce P-air electrodes increased the BET specific surface area from 95 to 106 m^2 g^{-1} and increased the adsorption capacity of the electrodes from 1.36 mg g^{-1} (untreated) to 2.40 mg g^{-1} (P-air) in Pb^{2+} solutions of 5 mg L^{-1} at a voltage of 450 mV.[127]

Electrodes made by electrodepositing reduced graphene oxide (rGO) on a SSN achieved an overall better performance compared to the SSN alone.[128] The advantage of synthesizing the composite electrode *via* electrodeposition *versus* using polymeric binders is that binders can destroy the electrode surface and increase its electrical resistance.[129] The rGO coating also provides high protection against corrosion and

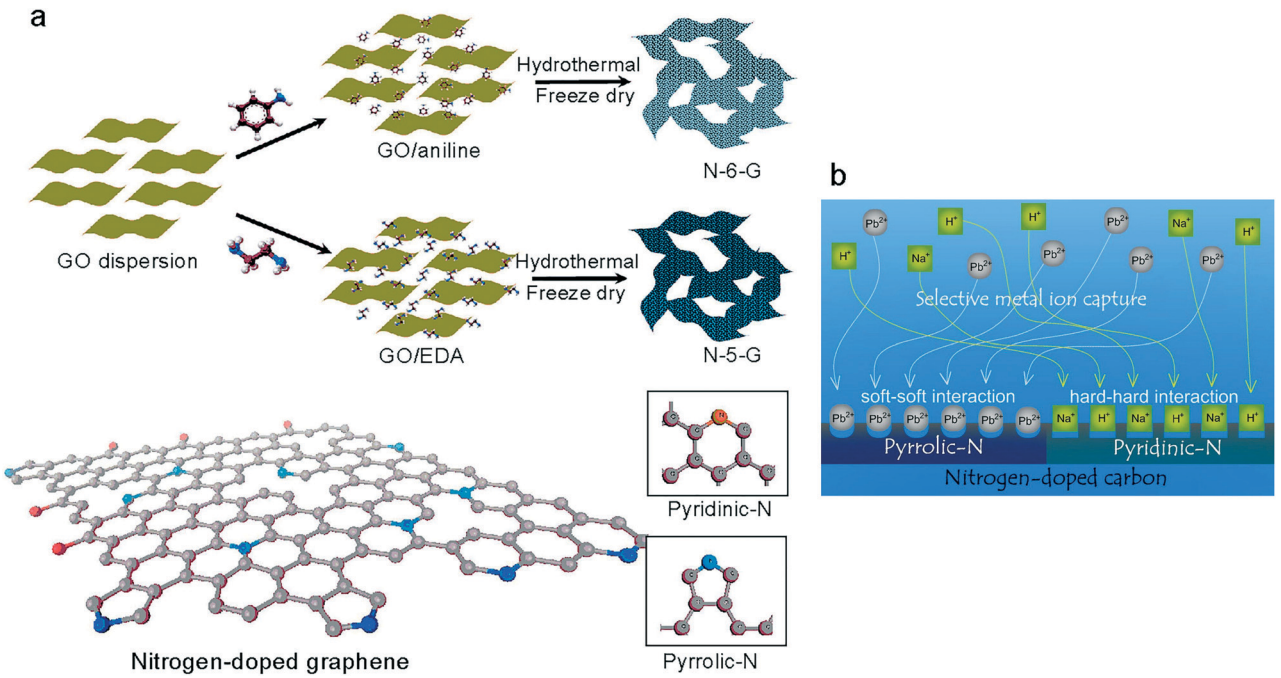

Fig. 5 Electrosorptive selectivity toward soft Pb^{2+} ions could be controlled by the amount of pyrrolic-N and pyridinic-N added to graphene electrodes. (a) The synthesis route using aniline produced electrodes with more pyridinic-N (N-6-G) while the synthetic route using ethylenediamine (EDA) produced electrodes with more pyrrolic-N (N-5-G). (b) The electrodes with a greater amount of soft pyrrolic-N (N-G-6) showed a greater affinity toward soft Pb^{2+} ions. Reproduced from ref. 125 with permission from Elsevier, copyright 2019.

supplies active sites for Pb^{2+} adsorption. This feature enhanced the effectiveness of rGO/SSN electrode for lead treatment in wastewater. The removal efficiency of rGO/SSN electrode reached 97.2% of 1000 mg Pb L^{-1}, which was about 12% higher than the SSN electrode, with a 4.45 times fasterremoval rate.[128]

Graphene aerogels (GAs), made from graphene oxide (GO), showed improved ability to remove Pb^{2+} when doped with nitrogen to make nitrogen-doped graphene aerogels (NGAs).[130] The NGAs could remove about 42% of the Pb^{2+} from a 1 mM Pb^{2+} (207 mg L^{-1}) solution at −0.3 V *vs.* SCE while the GAs could only remove about 39% of the Pb^{2+} and reduced graphene oxide (rGO) could only remove about 36% of the Pb^{2+} at the same conditions. The enhanced electrosorptive ability was attributed to the intrinsic charges on NGAs attracting Pb^{2+}, the greater surface area of the NGAs (434.4 m^2 g^{-1} for NGAs, 393.4 m^2 g^{-1} for GAs, and 16.9 m^2 g^{-1} for rGO), and coordination between doped nitrogen atoms and Pb^{2+}. These effects contributed to the NGAs high electrosorption capacity (650.4 mg g^{-1}). Crumpled nitrogen-doped graphene (CNG) nanosheets used for membrane-CDI (MCDI) achieved an electrosorption capacity of 521 mg g^{-1} Pb^{2+} from 200 ppm Pb^{2+} at 1.2 V.[99] This high electrosorption capacity was attributed to the CNG providing a large ion-accessible surface area, and a porous structure that created a highly conductive network and enabled fast ion transport. The N-doping also not only help create the crumpled structure, but the N dopants formed activated sites that could participate in the electrosorption of ions. Graphene oxide-bearing nickel foam (GO/NF) electrodes were also highly effective at removing Pb^{2+} and had an electrosorption capacity of 663 mg g^{-1} from an initial concentration of 100 mg L^{-1} at 1.2 V.[121] This GO/NF had a negative surface, and possessed many oxygen-containing functional groups which could adsorb Pb^{2+} even without the application of an electric field (193.5 mg g^{-1} at open circuit). X-ray photoelectron spectroscopy showed the relative area of hydroxyl-character carbon reduced from 26.98% of the total carbon before adsorption to 7.98% after adsorption of Pb^{2+}, suggesting that hydroxyl groups played an important role in complexingwith Pb^{2+}. This complexation, in addition to the electrostatic attraction from an applied electric field, helps explain the high electrosorption capacity of GO/NF.

2.7.3 Composite electrodes. Various composite electrodes have been derived from carbon materials with improved electrosorptive properties.[119,131] Reduced graphene oxide/titanate nanotubes (rGO/TNT) composite electrodes removed 241.65 mg g^{-1} Pb within 2 hours from an 80 ppm Pb solution at 1.2 V.[102] The RGO/TNT composite had a high BET surface area of 511.226 m^2 g^{-1}, and 99.83% of it was mesoporous. In addition, the RGO/TNT composite consists of many electron-rich functional group such as sp and sp^2 hybridized carbon, which had a high affinity for Pb^{2+}.[128] All these surface properties greatly enhanced the electrode's electrosorption performance.

2.7.4 Polymer electrodes. Functional materials such as conducting polymers are alternatives to carbon-based electrodes for use in capacitive deionization. Conductive

Table 7 Lead

Species	Electrode material	Specific surface area ($m^2 g^{-1}$)	Voltage/charge	Initial concentration	Percent of heavy metal removed	Electrosorption capacity (mg g^{-1})	Operation time	pH	Ref.
Pb(II)	Activated carbon (AC)	—	−0.13 V *vs.* SCE	5 mg L^{-1}	97.5%	17.71	—	5.0	120
Pb(II)	AC cloth	—	1.2 V	0.5 mM (104 mg L^{-1})	43%	—	120 min	5.0	13
Pb(II)	AC Fiber	—	1.4 V	155 mg L^{-1}	47.25%	191.66	300 min	7.0	132
Pb(II)	Three-dimensional graphene	2630	1.4 V	100 mg L^{-1}	99.9%	—	60 min	6.0	124
Pb(II)	Graphene–carbon nanotube hybrid aerogel	435	1.6 V	100 mg L^{-1}	—	44.5	120 min	6	133
	Acid treated graphene–carbon nanotube hybrid aerogel	365	1.6 V	100 mg L^{-1}	—	104.9	120 min	6	
Pb(II)	Pyrrolic N-dominated graphene	198	−1.2 V	0.4 μM	~100%	481.5	30 min	5.0	125
	Pyridinic N-dominated graphene	268	−1.2 V	0.4 μM	—	196.8	30 min	5.0	
Pb(II)	Nitrogen-doped graphene aerogel	434.4	−0.3 V *vs.* SCE	1 mM (207 mg L^{-1})	—	650.4	—	4.2	130
Pb(II)	Nitrogen-doped graphene nanosheet (MCDI)	695	1.2 V	200 ppm (200 mg L^{-1})	—	521	60 min	—	99
Pb(II)	Titanate nanotubes	240.2	1.2 V	100 mg L^{-1}	—	299.5	180 min	5.0	134
	Acid treated titanate nanotubes	—	1.2 V	100 mg L^{-1}	—	227.61	180 min	5.0	
Pb(II)	Reduced graphene oxide/titanate nanotubes	511.226	1.2 V	80 ppm (80 mg L^{-1})	—	241.65	120 min	—	102
Pb(II)	Graphene oxide with nickel foam	314.50	0 V	100 mg L^{-1}	—	193.5	60 min	5.0	121
	Graphene oxide with nickel foam	314.50	1.2 V	100 mg L^{-1}	—	663	60 min	5.0	
Pb(II)	Graphene/Fe_3O_4	380	1.6 V	500 mg L^{-1}	—	47	300 min	—	100
Pb(II)	Porous graphitic carbon nanosheets/Fe_3O_4	1692.6	1.2 V	20 mg L^{-1}	—	20.9	60 min	—	101
Pb(II)	Carbon nanotubes/polypyrrole	42	450 mV	10 mg L^{-1}	—	3.85	80 min	6	135
	Plasma activated carbon nanotubes/polypyrrole	80	450 mV	10 mg L^{-1}	—	4.28	80 min	6	
Pb(II)	Air-plasma treated carbon nanotube/polytetrafluoroethylene	106	450 mV	5 mg L^{-1}	—	2.4	120 min	—	127
Pb(II)	Single-walled carbon nanotubes/stainless steel net	380	−2.0 V *vs.* SCE	150 mg L^{-1}	99.6%	—	90 min	6.5	114
Pb(II)	Polyaniline/attapulgite composite	119	−0.3 V *vs.* SCE	0.1 mM (20.7 mg L^{-1})	—	15.42	10 min	—	136

polymers have attracted attention as electrode materials because of their unique properties such as high stability under ambient conditions and variable conductivity.[136] The hetero N atoms in polyaniline (PANI) are capable of removing Pb^{2+} ions through chelation.[137] A composite electrode using PANI and attapulgite (ATP), a natural clay mineral with a high specific surface area and known affinity for heavy metal ions, achieved an adsorption capacity of 15.42 mg g^{-1} with from 1 mM Pb^{2+} (207 mg L^{-1}) at −0.3 V *vs.* SCE after 10 minutes.[136] The removal of Pb^{2+} ions by PANI/ATP electrode was driven by a combination of the chelation reaction, electrostatic interactions, and the physisorption brought from ATP.

2.7.5 Effects of pH on Pb electrosorption. The pH of the contaminated solution can greatly affect the electrosorption of Pb^{2+}. Pb^{2+} capture using single wall CNT on stainless steel nets showed the highest Pb removal rates at pH 6.50 and the lowest removal rates at pH 2.00 across a tested range of pH 2–6.5.[114] Other experiments have shown the same pattern of decreased electrosorption at low pH. Across a range of pH 2 to pH 7, electrosorption using AC showed maximum efficiency at pH 5 with a removal efficiency of 97.55%.[115] The slow removal rate of Pb^{2+} ions at low pH was due to the competition between H_3O^+ and Pb^{2+} ions for adsorption sites.[114,120] In a low pH environment, the concentration of H_3O^+ ions is significantly greater than that of Pb^{2+} ions and as a result, most of the electrode surface is occupied by the H_3O^+ ions. As the pH increases, the concentration of H_3O^+ ions decreases, increasing the amount of exposed metal binding sites carrying negative charges, which attract more Pb^{2+} ions.[131] At higher pH (>6) precipitation of lead to form lead hydroxide inhibits adsorption.[115]

2.8 Uranium

Uranium is a significant component of nuclear energy production, and the development of nuclear energy has caused uranium to be widely released into the environment as hexavalent U(VI) ions.[138] The U(VI) ions pose a great threat towards the environmental health due to its high chemical and radiological toxicity. The WHO guideline value for

Table 8 Uranium

Species	Electrode material	Specific surface area (m^2 g^{-1})	Voltage/charge	Initial concentration	Percent of heavy metal removed	Electrosorption capacity (mg g^{-1})	Operation time	pH	Ref.
U(VI)	Phosphate functionalized graphene hydrogel	202.4	1.2 V	100 mg L^{-1}	—	534.4	60 min	5	138
U(VI)	Activated carbon fiber	999.5	5 V	10 mg L^{-1}	76%	3.8	480 min	—	139
U(VI)	Carbon fiber	25.7	−0.9 V *vs.* Ag/AgCl	100 mg L^{-1}	—	~500	48 h	3.5	140
U(VI)	Three-dimensional graphene	161.24	1.8 V	100 mg L^{-1}	—	113.8	150 min	5	123
U(VI)	Activated carbon and PVdF binder	50	0.8 V	0.003 mg L^{-1}		3.4	300 min		141

uranium in drinking water is 30 μg L^{-1} and the US EPA MCL for uranium in drinking water is also 30 μg L^{-1}.[34,53] Various uranium electrosorption results are listed in Table 8.

2.8.1 Carbon-based electrodes. Carbon-based materials are commonly used for uranium ion electrosorption because they have high specific surface areas, good electrical conductivity, and are inert to a wide variety of chemicals. A phosphate functionalized graphene hydrogel (HGP), made by activating graphene oxide with phosphate groups using phytic acid (PA), had a maximum adsorption capacity of 545.7 mg g^{-1} at 1.2 V and pH 5.0.[138] The hydrogels had an interconnected 3D network structure with hierarchical pores, which greatly increased their specific surface area. In addition to the high adsorption capacity, the electrode also achieved a high desorption ratio of 90.9% at *via* HNO_3 eluting at open circuit. The HGP electrodes removed more mg Pb per g than plain reduced graphene electrodes because the HGP electrodes included additional phosphate groups which captured Pb^{2+} *via* chemisorption.

Carbon fiber electrodes, produced by a catalytic vapor-deposition process, removed up to 99.85% of the uranium from a 100 mg L^{-1} uranium feed solution at −0.6 V *vs.* Ag/AgCl, which corresponded to an uptake of 1.2 g g^{-1}.[140] An AC fiber electrode (Osaka Gas Co., FN-200PS-15) removed more than 99% of the uranium present lagoon sludge containing 100 mg L^{-1} of uranium at pH 4 and −0.9 V *vs.* Ag/AgCl.[145] More than 99% of the adsorbed uranium was discharged at a potential of +1.2 V *vs.* Ag/AgCl and pH 3.

2.8.2 Composite electrodes. A half-wave rectified alternating current electrochemical (HW-ACE) method effectively removed uranium at low concentrations from seawater with an amidoxime functionalized carbon electrode.[146] The amidoxime electrode provided chelation sites that preferably bound with uranyl ions (UO_2^{2+}).[147] These chelation sites allow uranyl ions to selectively bind to the surface of the electrode and be reduced to charge neutral U(IV) species, such as UO_2. When the applied potential is released, UO_2 stays bound to the electrode while other ions are rejected into the solution again. Reapplying the potential adsorbs and reduces more uranyl ions and the UO_2 particles on the electrode surface grow. The HW-ACE method achieved a uranium extraction capacity of 1932 mg g^{-1}, which is ninefold higher than conventional physico-chemical methods.[146]

2.9 Vanadium

Vanadium is a rare heavy metal that can pose a serious threat to environmental health, especially in its most toxic form, V(v). Vanadium causes a variety of toxic effects including, but not limited to, hemolysis, embryotoxicity, and functional lesions in the liver and kidneys.[148] Vanadium mining and smelting has caused environmental pollution in countries such as Russia, China, and South Africa.[149] Vanadium containing wastewater commonly has high salinity and low biodegradability, making it difficult to treat by conventional methods. Adsorption-based techniques are therefore a promising field of research for processing V-containing wastewater.[150]

2.9.1 Carbon and composite electrodes. A high-area carbon cloth could remove about 80% of VO_3^- in a water sample upon the application of a 0.1 mA galvanostatic current.[151] CDI can also potentially be used in removing vanadium from the acid leaching solutions commonly used in vanadium extraction.[152] Electrodes containing ion exchange resins on activated carbon have been investigated for their ability to selectively recover vanadium from a complex acid leaching solution.[142–144] Out of three cation exchange resin/mineral active carbon electrodes tested for their ability to remove vanadium, the electrodes made from D860 cation exchange resin had the highest adsorption capacity at 15.67 mg g^{-1} VO^{2+} material from a solution containing 300 mg L^{-1} VO^{2+}, 300 mg L^{-1} Fe^{3+} and 300 mg L^{-1} Al^{3+} at an 1.5 V.[144] The D860/active carbon electrode was selective for VO^{2+} because VO^{2+} has a relatively high affinity for the resin material and a smaller hydrated radius compared to the hydrated radii of other metals present in the acid leaching solution, allowing it to pass through the pores of the electrode more easily. Additionally, the D860/active carbon electrode showed good regenerative ability. The same D860 resin on coconut shell activated carbon had a much higher capacity of about 170 mg V(v) per g material.[143] Replacing the D860 with an anion exchange resin (D314) made electrodes that could adsorb about 230 mg V(v) per g.[143] The electrosorption performance of electrodes made with different resins is listed in Table 9. The electrosorption these resin/active carbon electrodes did not change significantly when the applied voltage was changed between

Table 9 Vanadium

Species	Electrode material	Specific surface area (m^2 g^{-1})	Voltage/charge	Initial concentration	Percent of heavy metal removed	Electrosorption capacity (mg g^{-1})	Operation time	pH	Ref.
V(v)	Activated carbon (AC)	1027	1.0 V	1000 mg L^{-1}	—	75.3	120 min	2.5	142
	Resin-activated carbon composite	—	1.0 V	1000 mg L^{-1}	—	127.7	120 min	2.5	
V(v)	Ion-exchange resin (IER)-D201/AC	441 (BET)	0.2 V	1500 mg L^{-1}	—	~210	120 min	2.5	143
			1.2 V	1500 mg L^{-1}	—	~200			
	IER-D301/AC	380 (BET)	0.2 V	1500 mg L^{-1}	—	~195	120 min	2.5	
			1.2 V	1500 mg L^{-1}	—	~180			
	IER-D314/AC	443 (BET)	0.2 V	1500 mg L^{-1}	—	~230	120 min	2.5	
			1.2 V	1500 mg L^{-1}	—	~360			
	IER-D860/AC	434 (BET)	0.2 V	1500 mg L^{-1}	—	~170	120 min	2.0	
			1.2 V	1500 mg L^{-1}	—	~130			
V(iv)	Minerals activated carbon (AC-m)	42 (BET)	1.5 V	300 mg L^{-1}	—	12.11	60	2.0	144
	IER-D860/AC-m	228 (BET)	1.5 V	300 mg L^{-1}	—	26.63			
	IER-D860	—	1.5 V	300 mg L^{-1}		52.88			

0.2 V and 1.2 V, suggesting that physisorption and/or chemisorption dominated over electrosorption. The adsorption capacity of the anion exchange resin/active carbon electrodes decreased significantly at a pH of 1.5 because at low pH, cationic VO^{2+} is more prevalent than the anionic vanadium species that react with the resin.

2.10 Zinc

Zinc is essential for many enzymes, but in high enough levels it can cause health problems including impairment of the immune system, vomiting, and anemia.[83,153] Zinc contamination is prevalent in various parts of China due to zinc smelting activity.[154] To prevent the precipitation of $Zn(OH)_2$, Zn removal through electrosorptive means is generally carried out in acidic solutions.[153]

2.10.1 Activated carbon electrodes. AC from a wide variety of sources, including petroleum coke, coconut shell, and phenolic resin have been used in the electrosorptive removal of Zn (Table 10).[89,91] About 40% of Zn from a 100 mg L^{-1} solution was removed onto AC cloth after 1000 s under a potential of 1.2 V.[155] AC fiber electrodes showed a Zn^{2+} uptake of 122.6 mg g^{-1} from a 500 mg L^{-1} Zn^{2+} solution with a potential of 1.2 V.[87] Powdered banana peels treated with sulfuric acids were found to have a maximum adsorption capacity of ~3.4 mg g^{-1}.[156] Beyond AC, other forms of carbon such as a CNT/carbon nanofiber composite and N-doped graphene nanosheets have also been used as electrode materials in removing Zn^{2+}.[70,99]

2.10.2 Metal-oxide composite electrodes. Various forms of birnessite have been used as electrodes for zinc electrosorption (Table 10). Birnessite–CNT composites were able to adsorb up to 155.6 mg g^{-1} of Zn^{2+}.[112] The reduction of Mn(iv) in birnessite (MnO_2) to Mn(ii) and Mn(iii) allowed Zn to be captured as $ZnMn_2O_4$ (Fig. 6). The potential that maximized uptake was 0.0 V *vs.* SCE. While lowering the potential below 0.0 V *vs.* SCE would favor Zn^{2+} migration towards the electrode, these lower potentials increased in the formation of Mn_3O_4 rather than $ZnMn_2O_4$ on the electrode surface, which decreased Zn removal at lower potentials.

Table 10 Zinc

Species	Electrode material	Specific surface area (m^2 g^{-1})	Voltage/charge	Initial concentration	Percent of heavy metal removed	Electrosorption capacity (mg g^{-1})	Operation time	pH	Ref.
Zn(ii)	AC (AG-3V)	—	−0.67 V *vs.* Ag/AgCl	1000 mg L^{-1}	—	15	—	—	91
Zn(ii)	Birnessite (nanostructured)	118	Charge discharge cycles at 0.1 A g^{-1} birnessite and from 0–0.9 V	1400 mg L^{-1}	—	530	—	—	153
				200 mg L^{-1}	—	319.8			
Zn(ii)	Birnessite/CNT nanocomposites (45.6% MnO_2)	143	0 V *vs.* SCE	50 mg L^{-1}	—	158.4	12 h	—	112
Zn(ii)	Birnessite nanosheets	179	Charge–discharge cycles from −0.9 to 0.9 V	1400 mg L^{-1}	—	383.2	—	—	157
				200 mg L^{-1}	—	79.9			
Zn(ii)	AC cloth	1118	1.2 V	75 mg L^{-1}	~45%	—	1000 s	—	155
				100 mg L^{-1}	~40%	—	1000 s		
Zn(ii)	AC fiber	1384.2	1.2 V	500 mg L^{-1}	—	122.6		—	87

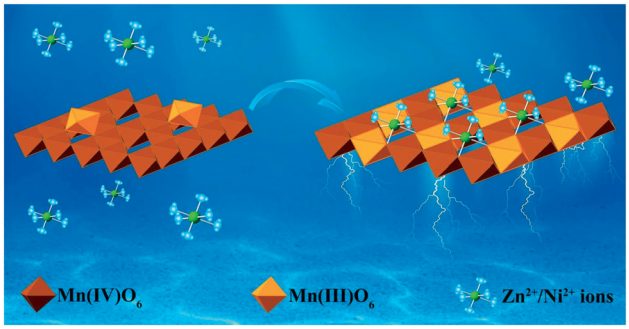

Fig. 6 Electrodes made from birnessite, a manganese oxide mineral, captured Zn^{2+} and Ni^{2+} by reducing the manganese within the birnessite from Mn(IV) to Mn(III). This reduction is accompanied by the insertion of Zn^{2+} or Ni^{2+} into the birnessite. Reproduced from ref. 112 with permission from Elsevier, copyright 2019.

Nanostructured birnessite had uptakes as high as 530 mg g^{-1} in a 1400 mg L^{-1} Zn^{2+} solution following a series of 50 charge–discharge cycles.[153] However, upon adsorption and insertion of Zn^{2+} into the birnessite electrodes, Mn^{2+} ions leached out of the birnessite. When used in a 1000 mg L^{-1} Zn^{2+} solution, the birnessite electrodes released 36.19% of the Mn they contained. Birnessite nanosheets could adsorb up to 383.2 mg g^{-1} following 50 charge–discharge cycles.[157] Increasing the current density during this process resulted in a decrease in the adsorption capacity. Fe_3O_4 on porous graphitic carbon nanosheets was able to remove Zn^{2+} along with several other metal cations.[101]

2.11 Other heavy metals and ions

While this review of electrosorption has focused on As, Cd, Cr, Cu, Fe, Ni, Pb, V, U, and Zn, in principle any liquid-phase ion can be captured using electrosorptive and capacitive deionization processes. Mercury can be removed *via* electrosorptive processes,[95,158] but this has not been extensively studied. Instead, mercury has been effectively removed *via* electrochemical alloy formation on platinum electrodes.[159] While not extensively studied, non-metal environmental contaminants such as selenium can be removed *via* electrosorption.[160] The man-made element technetium, mainly long-lived radioactive isotope Tc-99, has been introduced into the environment in increasing amounts due to the operation of nuclear fuel facilities and nuclear weapon testing.[161] Technetium-99 is of concern because it has a long half-life and, similar to many other heavy metals, it has high environmental mobility. Because Tc predominately exists as the oxyanion perrhenate TcO_4^-, it can also be removed *via* electrosorption.[162]

3. Concluding remarks and research directions

As presented in this review, there is a large and growing body of work investigating heavy metal removal using capacitive deionization and electrosorption. However, it can be noticed that there lacks, across the various sources, a unified or standard approach to studying electrode materials for heavy metal electrosorption. The traditional metrics that quantify electrosorption performance, adsorption uptake and percent removal, are not truly intensive; they are highly dependent upon the experimental variables like the initial concentration of ions, the volume of water used, and the electrode mass used. As a result, it can be misleading to directly compare reported adsorption uptake and percent removal between different studies. It may be more useful to directly compare Langmuir isotherm equilibrium constants, which fully define adsorption capacity as a function of equilibrium ion concentration. Using the Langmuir model constants would account for variations in some of the experimental parameters between different studies. While many studies already report adsorption model constants,[85,109,110] not all of them do. However, even this Langmuir descriptor cannot account for performance differences across different water matrices where different competing ions can take up adsorption capacity. Also, the Langmuir model is not always a suitable model for irregular surfaces such as AC electrode surfaces.[163] When comparing results between different studies, it is recommended that readers be aware of these shortcomings and take note of experimental parameters such as competing ion or supporting electrolyte concentration and pH.

In the interest of developing selective electrode materials, we suggest the inclusion of relative separation factors for studies that investigate selective materials for heavy metal electrosorption. The separation factor between two ions A and B, typically denoted as α, is defined as:[164]

$$\alpha_{A,B} = (N_{A,ads}/N_{B,ads})/(N_{A,l}/N_{B,l}) \quad (1)$$

where the N's indicate molar quantities and subscripts refer to A and B adsorbed (ads) or in the liquid phase (l). When multiple ions are present in solution, they compete for surface sites in reactions such as:

$$A + B_{ads} \underset{k_{-1}}{\overset{k_1}{\rightleftharpoons}} Aads + B \quad (2)$$

The separation factor, by definition, is exactly the equilibrium constant of this reaction:

$$K_{eq} = \frac{[A_{ads}][B]}{[A][B_{ads}]} = \frac{k_1}{k_{-1}} = \alpha \quad (3)$$

As a result, separation factors directly quantify the free energy difference of eqn (2) and could be used to quantify differences in affinity of the electrode with different heavy metal ions and other competing ions.

3.1 Ion selectivity

Several factors govern ion selectivity including ion radius, ion charge, and an ion's physicochemical affinity for the electrode. While ion selectivity is complex and system

dependent, a rule of thumb is that ions of higher charge are preferentially removed over ions of lower charge and between ions of the same charge, ions with smaller hydrated radii are preferentially removed. Individual removal experiments of Cr^{3+}, Cd^{2+}, and Pb^{2+} using AC cloth (ACC, FM70) showed the highest removal efficiency for Cr^{3+} (52.48% for Cr^{3+}, 42.62% for Pb^{2+}, 31.85% for Cd^{2+}) after 2 hours from 5 mM solutions at 1.2 V.[13] It was noted that at open circuit (0 V), Cr^{3+} and Pb^{2+} were still significantly adsorbed (41.52% removal for Cr^{3+}, 29.59% for Pb^{2+}) while Cd^{2+} was not (4.20% removal). These results suggest that Cr^{3+} and Pb^{2+} had some intrinsic affinity for the AC cloth and adsorbed much more quickly due to physical adsorption attractions. Between the three ions, Pb^{2+} has the smallest hydrated radius, followed by Cd^{2+}, then Cr^{3+}. Between Pb^{2+} and Cd^{2+}, Pb^{2+} is preferentially adsorbed because it has a smaller ionic radius. Despite having the largest hydrated radius, Cr^{3+} was preferentially adsorbed due to its higher charge. Nitrogen-doped graphene nanosheets, used to remove 9 different divalent cations (Pb^{2+}, Cu^{2+}, Fe^{2+}, Cd^{2+}, Co^{2+}, Ni^{2+}, Zn^{2+}, Mg^{2+}, Ca^{2+}) showed the quickest removal rate for Fe^{2+} and the slowest removal rate for Cd^{2+}.[99] This is consistent with the previously presented study. It was noted that Fe^{2+} was likely oxidized to Fe^{3+}, which allowed it to out compete all of the other divalent cations. Cd^{2+}, again, was least favorably adsorbed due to its larger hydrated radius. Electrosorption of Fe^{3+}, Cu^{2+}, Zn^{2+}, and Na^{+} using carbon nanotubes and carbon nanofibers (CNTs–CNFs) composite electrodes showed adsorption favoured $Fe^{3+} > Cu^{2+} > Zn^{2+} > Na^{+}$.[70] Again, this order can be explained by ion charge and hydrated radius. Overall, Fe^{3+} was preferentially adsorbed due to its high charge and Cu^{2+} adsorption was favoured over Zn^{2+} adsorption due to Cu^{2+} having a smaller hydrated radius.

Heteroatom doping of carbon materials has been shown to increase selectivity and/or electrosorption capacity for heavy metal ions. Graphene aerogels doped with sulfur (SGAs) had a higher electrosorption capacity than graphene aerogels doped with nitrogen (NGAs).[95] This was explained with the hard–soft-acid–base principle where sulfur, the softer heteroatom between sulfur and nitrogen, showed stronger interactions with soft heavy metal atoms. Not only does the identity of the heteroatom affect electrosorption, but the chemical environment of the heteroatom affects how it interacts with heavy metal ions. This was shown with graphene doped with nitrogen in two ways: the first forming more nitrogen with pyridinic character, and the second forming more nitrogen with pyrrolic character.[125] The pyridinic N-doped graphene showed greater affinity for hard ions (H^{+}, Na^{+}) while the pyrrolic N-doped character showed greater affinity for soft ions (Pb^{2+}).[125]

New faradaic electrode materials have been shown to selectively capture heavy metal ions. Poly(vinylferrocene), a redox-active metallopolymer, has been shown to selectively capture chromium and arsenic oxyanions over perchlorate and chloride competing ions.[40] When oxidized, the ferrocenium cations on the polymer act as adsorption sites and bind anions through charge transfer. Chromium and arsenic oxyanions were shown to bind strongly to poly(vinylferrocene) because these oxyanions are highly polarizable and willingly donate electron density toward the positive ferrocenium sites. Perchlorate and chloride were less polarizable and did not bind strongly to poly(vinylferrocene).

These studies have demonstrated the ability to tune ion selectivity through molecular modification and design. As the field of heavy metal electrosorption grows and differentiates itself from desalination work, we anticipate a greater focus on molecular design of selective electrosorbents and building an understanding for the mechanisms that govern ion selectivity.

3.2 Viability of electrosorption and capacitive deionization for heavy metal removal

Electrosorption and capacitive deionization have a bright future in applications for heavy metal capture. These processes are efficient for ion removal when ion concentrations are low, which is often the case for heavy metal contamination, and can be augmented with other ion removal techniques such as membrane processes.

Research on the commercial performance of CDI plants, especially when applied to heavy metal removal, is extremely limited.[165] However, CDI has the potential to be a highly energy-efficient method to remove heavy metal ions from water. For example, in applications other than heavy metal removal, such as desalination, CDI is projected to be more energy efficient than leading industrial technologies such as reverse osmosis for salt concentrations less than 60 mM.[166] The minimum energy required by CDI to reduce the total dissolved solids (TDS) in water from 1000 mg L^{-1} to 10 mg L^{-1} has been estimated to be as low as 0.1 kW h m^{-1}.[328] A bench-scale industrial-type process using a carbon aerogel electrode could achieve the same TDS reduction using 0.594 kW h m^{-3}, much lower than the 2.03 kW h m^{-3} required for electrodialysis reverse systems.[28] Additionally, the large-scale production of electrode materials such as AC and carbon aerogels has already been shown to be viable.[167] A key factor in the energy efficiency of CDI processes is the potential for energy recovery during the desorption stage. At low salt concentrations, energy recovery as high as 83% has been achieved in membrane CDI processes.[165] While these studies regarding the energy required for large-scale CDI processes suggest that CDI and electrosorption may be viable alternatives to other ion removal processes, more detailed technoeconomic analysis is required to determine if electrosorption of heavy metals is viable at a large scale. The viability of a large-scale heavy metal electrosorption process will depend upon electrode capacity, ion selectivity, electrode regeneration and stability, and energy recovery.

3.3 Future directions

A large fraction of the electrode materials covered in this review are porous carbon materials. These are prime candidatematerials

for electrosorption because they have high surface areas, and are inexpensive as well as widely available. However, heavy metal electrosorption research has started to move towards functionalizing carbon materials and designing new electrode materials to selectively target heavy metal ions in the presence of competing ions. Future directions in electrosorption of heavy metals are expected to shift towards heteroatom functionalization and more advanced faradaic materials, including ion-intercalation and ion-binding platforms.[21,168] Rather than storing charge in an electric double layer, these materials store charge by intercalating ions within a crystalline matrix, or binding ions onto polymeric site, and can thus enhance both adsorption capacity and selectivity.

Thus, both faradaic and non-faradaic composite materials are expected to grow in interest for heavy metal removal. Finally, a trend which we also expect is the integration of different treatment steps for various ions through the design of novel materials, which can reduce competitive adsorption and maximize process efficiency.

Conflicts of interest

There are no conflicts to declare.

Acknowledgements

The authors thank the startup financial support provided by the University of Illinois Urbana-Champaign and the Department of Chemical and Biomolecular Engineering, and the support of the National Science Foundation under CBET Grant #1931941.

Notes and references

1 J. H. Duffus, "Heavy metals" a meaningless term? (IUPAC Technical Report), *Pure Appl. Chem.*, 2002, **74**, 793.
2 L. Järup, Hazards of heavy metal contamination, *Br. Med. Bull.*, 2003, **68**, 167–182.
3 P. B. Tchounwou, C. G. Yedjou, A. K. Patlolla and D. J. Sutton, Heavy metal toxicity and the environment, *Exper. Suppl.*, 2012, **2012**(101), 133–164.
4 K. R. Mahaffey, P. E. Corneliussen, C. F. Jelinek and J. A. Fiorino, Heavy metal exposure from foods, *Environ. Health Perspect.*, 1975, **12**, 63–69.
5 F. Fu and Q. Wang, Removal of heavy metal ions from wastewaters: A review, *J. Environ. Manage.*, 2011, **92**, 407–418.
6 H. Eccles, Treatment of metal-contaminated wastes: why select a biological process?, *Trends Biotechnol.*, 1999, **17**, 462–465.
7 N. Li, J. An, X. Wang, H. Wang, L. Lu and Z. J. Ren, Resin-enhanced rolling activated carbon electrode for efficient capacitive deionization, *Desalination*, 2017, **419**, 20–28.
8 N. Abdullah, N. Yusof, W. J. Lau, J. Jaafar and A. F. Ismail, Recent trends of heavy metal removal from water/wastewater by membrane technologies, *J. Ind. Eng. Chem.*, 2019, **76**, 17–38.
9 F. Liu, G. Zhang, Q. Meng and H. Zhang, Performance of Nanofiltration and Reverse Osmosis Membranes in Metal Effluent Treatment, *Chin. J. Chem. Eng.*, 2008, **16**, 441–445.
10 H. Wang and Z. J. Ren, Bioelectrochemical metal recovery from wastewater: A review, *Water Res.*, 2014, **66**, 219–232.
11 P. Kajitvichyanukul, J. Ananpattarachai and S. Pongpom, Sol–gel preparation and properties study of TiO2 thin film for photocatalytic reduction of chromium(VI) in photocatalysis process, *Sci. Technol. Adv. Mater.*, 2005, **6**, 352–358.
12 E. Gkika, A. Troupis, A. Hiskia and E. Papaconstantinou, Photocatalytic reduction of chromium and oxidation of organics by polyoxometalates, *Appl. Catal., B*, 2006, **62**, 28–34.
13 Z. Huang, L. Lu, Z. Cai and Z. J. Ren, Individual and competitive removal of heavy metals using capacitive deionization, *J. Hazard. Mater.*, 2016, **302**, 323–331.
14 Y. Oren, Capacitive deionization (CDI) for desalination and water treatment — past, present and future (a review), *Desalination*, 2008, **228**, 10–29.
15 M. E. Suss, S. Porada, X. Sun, P. M. Biesheuvel, J. Yoon and V. Presser, Water desalination via capacitive deionization: what is it and what can we expect from it?, *Energy Environ. Sci.*, 2015, **8**, 2296–2319.
16 X. Su and T. A. Hatton, Electrosorption, *Kirk-Othmer Encyclopedia of Chemical Technology*, 2016, pp. 1–11, DOI: 10.1002/0471238961.koe00022.
17 A. J. Bard and L. R. Faulkner, *Electrochemical methods: fundamentals and applications*, Wiley, New York, 2nd edn, 2001.
18 J. Kang, T. Kim, H. Shin, J. Lee, J.-I. Ha and J. Yoon, Direct energy recovery system for membrane capacitive deionization, *Desalination*, 2016, **398**, 144–150.
19 M. D. Ward, Ion Exchange of Ferro(ferri)cyanide in Polyvinylferrocene Films, *J. Electrochem. Soc.*, 1988, **135**, 2747–2750.
20 Y. Zhang, Q. Xue, F. Li and J. Dai, Removal of heavy metal ions from wastewater by capacitive deionization using polypyrrole/chitosan composite electrode, *Adsorpt. Sci. Technol.*, 2019, **37**, 205–216.
21 M. E. Suss and V. Presser, Water Desalination with Energy Storage Electrode Materials, *Joule*, 2018, **2**, 10–15.
22 J. Lee, S. Kim, C. Kim and J. Yoon, Hybrid capacitive deionization to enhance the desalination performance of capacitive techniques, *Energy Environ. Sci.*, 2014, **7**, 3683–3689.
23 J. Lee, P. Srimuk, R. L. Zornitta, M. Aslan, B. L. Mehdi and V. Presser, High Electrochemical Seawater Desalination Performance Enabled by an Iodide Redox Electrolyte Paired with a Sodium Superionic Conductor, *ACS Sustainable Chem. Eng.*, 2019, **7**, 10132–10142.
24 C. Kim, P. Srimuk, J. Lee and V. Presser, Enhanced desalination via cell voltage extension of membrane capacitive deionization using an aqueous/organic bi-electrolyte, *Desalination*, 2018, **443**, 56–61.

25 H. Yoon, J. Lee, S. Kim and J. Yoon, Hybrid capacitive deionization with Ag coated carbon composite electrode, *Desalination*, 2017, **422**, 42–48.
26 C. Zhao, L. Zhang, R. Ge, A. Zhang, C. Zhang and X. Chen, Treatment of low-level Cu(II) wastewater and regeneration through a novel capacitive deionization-electrodeionization (CDI-EDI) technology, *Chemosphere*, 2019, **217**, 763–772.
27 C. Forrestal, P. Xu and Z. Ren, Sustainable desalination using a microbial capacitive desalination cell, *Energy Environ. Sci.*, 2012, **5**, 7161–7167.
28 M. A. Anderson, A. L. Cudero and J. Palma, Capacitive deionization as an electrochemical means of saving energy and delivering clean water. Comparison to present desalination practices: Will it compete?, *Electrochim. Acta*, 2010, **55**, 3845–3856.
29 S. Kim, H. Yoon, D. Shin, J. Lee and J. Yoon, Electrochemical selective ion separation in capacitive deionization with sodium manganese oxide, *J. Colloid Interface Sci.*, 2017, **506**, 644–648.
30 X. Su and T. A. Hatton, Electrosorption at functional interfaces: from molecular-level interactions to electrochemical cell design, *Phys. Chem. Chem. Phys.*, 2017, **19**, 23570–23584.
31 X. Su and T. A. Hatton, Redox-electrodes for selective electrochemical separations, *Adv. Colloid Interface Sci.*, 2017, **244**, 6–20.
32 R. Singh, S. Singh, P. Parihar, V. P. Singh and S. M. Prasad, Arsenic contamination, consequences and remediation techniques: A review, *Ecotoxicol. Environ. Saf.*, 2015, **112**, 247–270.
33 *Technical Fact Sheet: Final Rules for Arsenic in Drinking Water*, Environmental Protection Agency, 2001.
34 World Health Organization, *Guidelines for Drinking-water Quality*, World Health Organization, Geneva, 4th edn, 2011.
35 M. F. Hughes, Arsenic toxicity and potential mechanisms of action, *Toxicol. Lett.*, 2002, **133**, 1–16.
36 Y. Lee, I.-H. Um and J. Yoon, Arsenic(III) Oxidation by Iron(VI) (Ferrate) and Subsequent Removal of Arsenic(V) by Iron(III) Coagulation, *Environ. Sci. Technol.*, 2003, **37**, 5750–5756.
37 E. Terlecka, Arsenic Speciation Analysis in Water Samples: A Review of The Hyphenated Techniques, *Environ. Monit. Assess.*, 2005, **107**, 259–284.
38 M. Dai, L. Xia, S. Song, C. Peng, J. R. Rangel-Mendez and R. Cruz-Gaona, Electrosorption of As(III) in aqueous solutions with activated carbon as the electrode, *Appl. Surf. Sci.*, 2018, **434**, 816–821.
39 C.-S. Fan, S.-C. Tseng, K.-C. Li and C.-H. Hou, Electro-removal of arsenic(III) and arsenic(V) from aqueous solutions by capacitive deionization, *J. Hazard. Mater.*, 2016, **312**, 208–215.
40 X. Su, A. Kushima, C. Halliday, J. Zhou, J. Li and T. A. Hatton, Electrochemically-mediated selective capture of heavy metal chromium and arsenic oxyanions from water, *Nat. Commun.*, 2018, **9**, 4701.
41 E. J. Bain, J. M. Calo, R. Spitz-Steinberg, J. Kirchner and J. Axen, Electrosorption/Electrodesorption of Arsenic on a Granular Activated Carbon in the Presence of Other Heavy Metals, *Energy Fuels*, 2010, **24**, 3415–3421.
42 J.-M. Beralus, R. Ruiz-Rosas, D. Cazorla-Amorós and E. Morallón, Electroadsorption of Arsenic from Natural Water in Granular Activated Carbon, *Front. Mater.*, 2014, **1**, 28.
43 M. Dai, M. Zhang, L. Xia, Y. Li, Y. Liu and S. Song, Combined Electrosorption and Chemisorption of As(V) in Water by Using Fe-rGO@AC Electrode, *ACS Sustainable Chem. Eng.*, 2017, **5**, 6532–6538.
44 C.-S. Fan, S. Y. H. Liou and C.-H. Hou, Capacitive deionization of arsenic-contaminated groundwater in a single-pass mode, *Chemosphere*, 2017, **184**, 924–931.
45 J.-Y. Lee, N. Chaimongkalayon, J. Lim, H. Y. Ha and S.-H. Moon, Arsenic removal from groundwater using low-cost carbon composite electrodes for capacitive deionization, *Water Sci. Technol.*, 2016, **73**, 3064–3071.
46 L. Peng, Y. Chen, H. Dong, Q. Zeng, H. Song, L. Chai and J.-D. Gu, Removal of Trace As(V) from Water with the Titanium Dioxide/ACF Composite Electrode, *Water, Air, Soil Pollut.*, 2015, **226**, 203.
47 Y. Song, Y. Wang, W. Mao, H. Sui, L. Yong, D. Yang, D. Jiang, L. Zhang and Y. Gong, Dietary cadmium exposure assessment among the Chinese population, *PLoS One*, 2017, **12**, e0177978.
48 P. G. Tucker, *Agency for Toxic Substances and Disease Registry: Case Studies in Environmental Medicine (CSEM) Cadmium Toxicity*, 2008.
49 S. Cai, L. Yue, Q. Shang and G. Nordberg, Cadmium exposure among residents in an area contaminated by irrigation water in China, *Bull. W. H. O.*, 1995, **73**, 359–367.
50 R. W. Simmons, P. Pongsakul, D. Saiyasitpanich and S. Klinphoklap, Elevated Levels of Cadmium and Zinc in Paddy Soils and Elevated Levels of Cadmium in Rice Grain Downstream of a Zinc Mineralized Area in Thailand: Implications for Public Health, *Environ. Geochem. Health*, 2005, **27**, 501–511.
51 J. M. R. S. Bandara, D. M. A. N. Senevirathna, D. M. R. S. B. Dasanayake, V. Herath, J. M. R. P. Bandara, T. Abeysekara and K. H. Rajapaksha, Chronic renal failure among farm families in cascade irrigation systems in Sri Lanka associated with elevated dietary cadmium levels in rice and freshwater fish (Tilapia), *Environ. Geochem. Health*, 2008, **30**, 465–478.
52 A. A. Meharg, G. Norton, C. Deacon, P. Williams, E. E. Adomako, A. Price, Y. Zhu, G. Li, F.-J. Zhao, S. McGrath, A. Villada, A. Sommella, P. M. C. S. De Silva, H. Brammer, T. Dasgupta and M. R. Islam, Variation in Rice Cadmium Related to Human Exposure, *Environ. Sci. Technol.*, 2013, **47**, 5613–5618.
53 National Primary Drinking Water Regulations, https://www.epa.gov/ground-water-and-drinking-water/national-primary-drinking-water-regulations, (accessed August 2019).
54 D. I. Marmanis, D. Konstantinos, A. K. Christoforidis and K. G. Ouzounis, Cadmium Removal From Aqueous Solution

by Capacitive Deionization with Nano - Porous Carbon Electrodes, *J. Eng. Sci. Technol. Rev.*, 2013, **6**, 165–166.

55 Y. Chen, L. Peng, Q. Zeng, Y. Yang, M. Lei, H. Song, L. Chai and J. Gu, Removal of trace Cd(II) from water with the manganese oxides/ACF composite electrode, *Clean Technol. Environ. Policy*, 2015, **17**, 49–57.

56 Q. Peng, L. Liu, Y. Luo, Y. Zhang, W. Tan, F. Liu, S. L. Suib and G. Qiu, Cadmium Removal from Aqueous Solution by a Deionization Supercapacitor with a Birnessite Electrode, *ACS Appl. Mater. Interfaces*, 2016, **8**, 34405–34413.

57 A. D. Dayan and A. J. Paine, Mechanisms of chromium toxicity, carcinogenicity and allergenicity: Review of the literature from 1985 to 2000, *Hum. Exp. Toxicol.*, 2001, **20**, 439–451.

58 G. Choppala, N. Bolan and J. H. Park, in *Advances in Agronomy*, ed. D. L. Sparks, Academic Press, 2013, vol. 120, pp. 129–172.

59 C. E. Barrera-Diaz, V. Lugo-Lugo and B. Bilyeu, A review of chemical, electrochemical and biological methods for aqueous Cr(VI) reduction, *J. Hazard. Mater.*, 2012, **223–224**, 1–12.

60 F. C. Richard and A. C. M. Bourg, Aqueous geochemistry of chromium: A review, *Water Res.*, 1991, **25**, 807–816.

61 P. Rana-Madaria, M. Nagarajan, C. Rajagopal and B. S. Garg, Removal of Chromium from Aqueous Solutions by Treatment with Carbon Aerogel Electrodes Using Response Surface Methodology, *Ind. Eng. Chem. Res.*, 2005, **44**, 6549–6559.

62 X. Zhao, B. Jia, Q. Sun, G. Jiao, L. Liu and D. She, Removal of Cr6+ ions from water by electrosorption on modified activated carbon fibre felt, *R. Soc. Open Sci.*, 2018, **5**, 180472.

63 M. Ziati, F. Khemmari, M. Kecir and S. Hazourli, Removal of chromium from tannery wastewater by electro-sorption on carbon prepared from peach stones: effect of applied potential, *Carbon Lett.*, 2017, **21**, 81–85.

64 X. F. Zhang, B. Wang, J. Yu, X. N. Wu, Y. H. Zang, H. C. Gao, P. C. Su and S. Q. Hao, Three-dimensional honeycomb-like porous carbon derived from corncob for the removal of heavy metals from water by capacitive deionization, *RSC Adv.*, 2018, **8**, 1159–1167.

65 P. Mohanraj, J. S. S. AllwinEbinesar, J. Amala and S. Bhuvaneshwari, Biocomposite based electrode for effective removal of Cr (VI) heavy metal via capacitive deionization, *Chem. Eng. Commun.*, 2019, DOI: 10.1080/00986445.2019.1627338.

66 M. S. Gaikwad and C. Balomajumder, Simultaneous electrosorptive removal of chromium(VI) and fluoride ions by capacitive deionization (CDI): Multicomponent isotherm modeling and kinetic study, *Sep. Purif. Technol.*, 2017, **186**, 272–281.

67 M. S. Gaikwad and C. Balomajumder, Tea waste biomass activated carbon electrode for simultaneous removal of Cr(VI) and fluoride by capacitive deionization, *Chemosphere*, 2017, **184**, 1141–1149.

68 M. S. Gaikwad and C. Balomajumder, Removal of Cr(VI) and fluoride by membrane capacitive deionization with nanoporous and microporous Limonia acidissima (wood apple) shell activated carbon electrode, *Sep. Purif. Technol.*, 2018, **195**, 305–313.

69 J. C. Farmer, S. M. Bahowick, J. E. Harrar, D. V. Fix, R. E. Martinelli, A. K. Vu and K. L. Carroll, Electrosorption of Chromium Ions on Carbon Aerogel Electrodes as a Means of Remediating Ground Water, *Energy Fuels*, 1997, **11**, 337–347.

70 Y. Gao, L. Pan, H. Li, Y. Zhang, Z. Zhang, Y. Chen and Z. Sun, Electrosorption behavior of cations with carbon nanotubes and carbon nanofibres composite film electrodes, *Thin Solid Films*, 2009, **517**, 1616–1619.

71 H. Wang and C. Na, Binder-Free Carbon Nanotube Electrode for Electrochemical Removal of Chromium, *ACS Appl. Mater. Interfaces*, 2014, **6**, 20309–20316.

72 Y.-X. Liu, D.-X. Yuan, J.-M. Yan, Q.-L. Li and T. Ouyang, Electrochemical removal of chromium from aqueous solutions using electrodes of stainless steel nets coated with single wall carbon nanotubes, *J. Hazard. Mater.*, 2011, **186**, 473–480.

73 S. Hou, X. Xu, M. Wang, T. Lu, C. Q. Sun and L. Pan, Synergistic conversion and removal of total Cr from aqueous solution by photocatalysis and capacitive deionization, *Chem. Eng. J.*, 2018, **337**, 398–404.

74 Y. Yan, F. Xue, F. Muhammad, L. Yu, F. Xu, B. Jiao, Y. Shiau and D. Li, Application of iron-loaded activated carbon electrodes for electrokinetic remediation of chromium-contaminated soil in a three-dimensional electrode system, *Sci. Rep.*, 2018, **8**, 5753.

75 X. Su, J. Hübner, M. J. Kauke, L. Dalbosco, J. Thomas, C. C. Gonzalez, E. Zhu, M. Franzreb, T. F. Jamison and T. A. Hatton, Redox Interfaces for Electrochemically Controlled Protein–Surface Interactions: Bioseparations and Heterogeneous Enzyme Catalysis, *Chem. Mater.*, 2017, **29**, 5702–5712.

76 X. Su, L. Bromberg, K.-J. Tan, T. F. Jamison, L. P. Padhye and T. A. Hatton, Electrochemically Mediated Reduction of Nitrosamines by Hemin-Functionalized Redox Electrodes, *Environ. Sci. Technol. Lett.*, 2017, **4**, 161–167.

77 X. Su, H. J. Kulik, T. F. Jamison and T. A. Hatton, Anion-Selective Redox Electrodes: Electrochemically Mediated Separation with Heterogeneous Organometallic Interfaces, *Adv. Funct. Mater.*, 2016, **26**, 3394–3404.

78 X. Su, K.-J. Tan, J. Elbert, C. Rüttiger, M. Gallei, T. F. Jamison and T. A. Hatton, Asymmetric Faradaic systems for selective electrochemical separations, *Energy Environ. Sci.*, 2017, **10**, 1272–1283.

79 J. Lee, P. Srimuk, S. Fleischmann, X. Su, T. A. Hatton and V. Presser, Redox-electrolytes for non-flow electrochemical energy storage: A critical review and best practice, *Prog. Mater. Sci.*, 2019, **101**, 46–89.

80 T. Winter, X. Su, T. A. Hatton and M. Gallei, Ferrocene-Containing Inverse Opals by Melt-Shear Organization of Core/Shell Particles, *Macromol. Rapid Commun.*, 2018, **39**, 1800428.

81 C.-C. Huang and Y.-J. Su, Removal of copper ions from wastewater by adsorption/electrosorption on modified

activated carbon cloths, *J. Hazard. Mater.*, 2010, **175**, 477–483.
82 *Copper in Drinking-water*, World Health Organization, 2004.
83 S. B. Goldhaber, Trace element risk assessment: essentiality vs. toxicity, *Regul. Toxicol. Pharmacol.*, 2003, **38**, 232–242.
84 C.-C. Huang and J.-C. He, Electrosorptive removal of copper ions from wastewater by using ordered mesoporous carbon electrodes, *Chem. Eng. J.*, 2013, **221**, 469–475.
85 C. Hu, F. Liu, H. Lan, H. Liu and J. Qu, Preparation of a manganese dioxide/carbon fiber electrode for electrosorptive removal of copper ions from water, *J. Colloid Interface Sci.*, 2015, **446**, 359–365.
86 W. Jin and M. Hu, High-Performance Capacitive Deionization of Copper Ions at Nanoporous ZnS-Decorated Carbon Felt, *J. Electrochem. Soc.*, 2019, **166**, E29–E34.
87 C. Wang, L. Chen and S. Liu, Activated carbon fiber for adsorption/electrodeposition of Cu (II) and the recovery of Cu (0) by controlling the applied voltage during membrane capacitive deionization, *J. Colloid Interface Sci.*, 2019, **548**, 160–169.
88 Y. Li, T. C. Stewart and H. L. Tang, A comparative study on electrosorptive rates of metal ions in capacitive deionization, *J. Water Process Eng.*, 2018, **26**, 257–263.
89 H. Oda and Y. Nakagawa, Removal of ionic substances from dilute solution using activated carbon electrodes, *Carbon*, 2003, **41**, 1037–1047.
90 S.-Y. Huang, C.-S. Fan and C.-H. Hou, Electro-enhanced removal of copper ions from aqueous solutions by capacitive deionization, *J. Hazard. Mater.*, 2014, **278**, 8–15.
91 M. M. Goldin, A. G. Volkov and D. N. Namychkin, Adsorption of Copper, Silver, and Zinc Cations on Polarized Activated Carbons, *J. Electrochem. Soc.*, 2005, **152**, E167.
92 T.-Y. Ying, K.-L. Yang, S. Yiacoumi and C. Tsouris, Electrosorption of Ions from Aqueous Solutions by Nanostructured Carbon Aerogel, *J. Colloid Interface Sci.*, 2002, **250**, 18–27.
93 Z. Cao, C. Zhang, Z. Yang, Q. Qin, Z. Zhang, X. Wang and J. Shen, Preparation of Carbon Aerogel Electrode for Electrosorption of Copper Ions in Aqueous Solution, *Materials*, 2019, **12**, 1864.
94 J. Li, X. Wang, H. Wang, S. Wang, T. Hayat, A. Alsaedi and X. Wang, Functionalization of biomass carbonaceous aerogels and their application as electrode materials for electro-enhanced recovery of metal ions, *Environ. Sci.: Nano*, 2017, **4**, 1114–1123.
95 Y. Wei, L. Xu, K. Yang, Y. Wang, Z. Wang, Y. Kong and H. Xue, Electrosorption of Toxic Heavy Metal Ions by Mono S- or N-Doped and S, N-Codoped 3D Graphene Aerogels, *J. Electrochem. Soc.*, 2017, **164**, E17–E22.
96 C.-C. Huang and S.-F. Siao, Removal of copper ions from an aqueous solution containing a chelating agent by electrosorption on mesoporous carbon electrodes, *J. Taiwan Inst. Chem. Eng.*, 2018, **85**, 29–39.
97 Y. Gao, H. B. Li, Z. J. Cheng, M. C. Zhang, Y. P. Zhang, Z. J. Zhang, Y. W. Chen, L. K. Pan and Z. Sun, *2008 2nd IEEE International Nanoelectronics Conference*, 2008.
98 Y. K. Zhan, H. Li, L. Pan, Y. Zhang, Y. Chen and Z. Sun, Regeneration of carbon nanotube and nanofibre composite film electrode for electrical removal of cupric ions, *Water Sci. Technol.*, 2010, **61**, 1427–1432.
99 L. Liu, X. Guo, R. Tallon, X. Huang and J. Chen, Highly porous N-doped graphene nanosheets for rapid removal of heavy metals from water by capacitive deionization, *Chem. Commun.*, 2017, **53**, 881–884.
100 G. Bharath, E. Alhseinat, N. Ponpandian, M. A. Khan, M. R. Siddiqui, F. Ahmed and E. H. Alsharaeh, Development of adsorption and electrosorption techniques for removal of organic and inorganic pollutants from wastewater using novel magnetite/porous graphene-based nanocomposites, *Sep. Purif. Technol.*, 2017, **188**, 206–218.
101 C. Zhao, X. Wang, S. Zhang, N. Sun, H. Zhou, G. Wang, Y. Zhang, H. Zhang and H. Zhao, Porous carbon nanosheets functionalized with Fe3O4 nanoparticles for capacitive removal of heavy metal ions from water, *Environ. Sci.: Water Res. Technol.*, 2020, DOI: 10.1039/C9EW00472F.
102 L. Bautista-Patacsil, J. P. L. Lazarte, R. C. Dipasupil, G. Y. Pasco, R. C. Eusebio, A. Orbecido and R. Doong, Deionization utilizing reduced graphene oxide-titanium dioxide nanotubes composite for the removal of Pb2+ and Cu2+, *J. Environ. Chem. Eng.*, 2019, 103063, DOI: 10.1016/j.jece.2019.103063.
103 X. Yang, L. Liu, W. Tan, G. Qiu and F. Liu, High-performance Cu2+ adsorption of birnessite using electrochemically controlled redox reactions, *J. Hazard. Mater.*, 2018, **354**, 107–115.
104 Y. Kong, W. Li, Z. Wang, C. Yao and Y. Tao, Electrosorption behavior of copper ions with poly(m-phenylenediamine) paper electrode, *Electrochem. Commun.*, 2013, **26**, 59–62.
105 K. Li, D. Guo, F. Lin, Y. Wei, W. Liu and Y. Kong, Electrosorption of copper ions by poly(m-phenylenediamine)/reduced graphene oxide synthesized via a one-step in situ redox strategy, *Electrochim. Acta*, 2015, **166**, 47–53.
106 Y.-J. Zhang, J.-Q. Xue, F. Li, J.-Z. Dai and X.-Z.-Y. Zhang, Preparation of polypyrrole/chitosan/carbon nanotube composite nano-electrode and application to capacitive deionization process for removing Cu2+, *Chem. Eng. Process.*, 2019, **139**, 121–129.
107 Y. Song, A. Kong, Y. Ji, B. He, H. Wang and J. Li, Adsorption for copper(II) ion with chitosan-SP/PET composite adsorbent enhanced by electric field, *Adsorpt. Sci. Technol.*, 2019, **37**, 274–287.
108 D. Ityel, Ground water: Dealing with iron contamination, *Filtr. Sep.*, 2011, **48**, 26–28.
109 H. Li, L. Zou, L. Pan and Z. Sun, Using graphene nano-flakes as electrodes to remove ferric ions by capacitive deionization, *Sep. Purif. Technol.*, 2010, **75**, 8–14.
110 S. Iftekhar, M. U. Farooq, M. Sillanpää, M. B. Asif and R. Habib, Removal of Ni(II) Using Multi-walled Carbon Nanotubes Electrodes: Relation Between Operating Parameters and Capacitive Deionization Performance, *Arabian J. Sci. Eng.*, 2017, **42**, 235–240.

111 P. Li, Y. Gui and D. J. Blackwood, Development of a Nanostructured alpha-MnO2/Carbon Paper Composite for Removal of Ni2+/Mn2+ Ions by Electrosorption, *ACS Appl. Mater. Interfaces*, 2018, **10**, 19615–19625.

112 L. Liu, G. Qiu, S. L. Suib, F. Liu, L. Zheng, W. Tan and L. Qin, Enhancement of Zn2+ and Ni2+ removal performance using a deionization pseudocapacitor with nanostructured birnessite and its carbon nanotube composite electrodes, *Chem. Eng. J.*, 2017, **328**, 464–473.

113 *Nickel in Drinking-water*, World Health Organization, 2005.

114 Y. Liu, J. Yan, D. Yuan, Q. Li and X. Wu, The study of lead removal from aqueous solution using an electrochemical method with a stainless steel net electrode coated with single wall carbon nanotubes, *Chem. Eng. J.*, 2013, **218**, 81–88.

115 K. Kordas, J. Ravenscroft, Y. Cao and E. V. McLean, Lead Exposure in Low and Middle-Income Countries: Perspectives and Lessons on Patterns, Injustices, Economics, and Politics, *Int. J. Environ. Res. Public Health*, 2018, **15**, 2351.

116 B. Fraser, La Oroya's Legacy of Lead, *Environ. Sci. Technol.*, 2009, **43**, 5555–5557.

117 J. Smith, *Mexican City Awakes to an Ecological Nightmare*, Los Angeles Times, 1999.

118 B. Anna, M. Kleopas, S. Constantine, F. Anestis and B. Maria, Adsorption of Cd(II), Cu(II), Ni(II) and Pb(II) onto natural bentonite: study in mono- and multi-metal systems, *Environ. Earth Sci.*, 2015, **73**, 5435–5444.

119 L. M. Chang, X. Y. Duan and W. Liu, Preparation and electrosorption desalination performance of activated carbon electrode with titania, *Desalination*, 2011, **270**, 285–290.

120 M. Ziati and S. Hazourli, Experimental investigation of activated carbon prepared from date stones adsorbent electrode for electrosorption of lead from aqueous solution, *Microchem. J.*, 2019, **146**, 164–169.

121 J. Zheng, L. Xia and S. Song, Electrosorption of Pb(ii) in water using graphene oxide-bearing nickel foam as the electrodes, *RSC Adv.*, 2017, **7**, 23543–23549.

122 D. Zhang, X. Wen, L. Shi, T. Yan and J. Zhang, Enhanced capacitive deionization of graphene/mesoporous carbon composites, *Nanoscale*, 2012, **4**, 5440–5446.

123 X. Wu, K. Li, S. Ying, L. Liu, M. Wang and Y. Liao, Three-dimensional graphene materials for UO22+ electrosorption, *J. Radioanal. Nucl. Chem.*, 2019, **321**, 977–984.

124 P. Liu, T. Yan, J. Zhang, L. Shi and D. Zhang, Separation and recovery of heavy metal ions and salt ions from wastewater by 3D graphene-based asymmetric electrodes via capacitive deionization, *J. Mater. Chem. A*, 2017, **5**, 14748–14757.

125 Q. Ji, C. Hu, H. Liu and J. Qu, Development of nitrogen-doped carbon for selective metal ion capture, *Chem. Eng. J.*, 2018, **350**, 608–615.

126 Y.-H. Li, S. Wang, J. Wei, X. Zhang, C. Xu, Z. Luan, D. Wu and B. Wei, Lead adsorption on carbon nanotubes, *Chem. Phys. Lett.*, 2002, **357**, 263–266.

127 L. Yang, Z. Shi and W. Yang, Enhanced capacitive deionization of lead ions using air-plasma treated carbon nanotube electrode, *Surf. Coat. Technol.*, 2014, **251**, 122–127.

128 X. Li, H. Li, X. Xu, N. Guo, L. Yuan and H. Yu, Preparation of a Reduced Graphene Oxide @ Stainless Steel Net Electrode and Its Application of Electrochemical Removal Pb(II), *J. Electrochem. Soc.*, 2017, **164**, E71–E77.

129 K.-K. Park, J.-B. Lee, P.-Y. Park, S.-W. Yoon, J.-S. Moon, H.-M. Eum and C.-W. Lee, Development of a carbon sheet electrode for electrosorption desalination, *Desalination*, 2007, **206**, 86–91.

130 Y. Wei, L. Xu, Y. Tao, C. Yao, H. Xue and Y. Kong, Electrosorption of Lead Ions by Nitrogen-Doped Graphene Aerogels via One-Pot Hydrothermal Route, *Ind. Eng. Chem. Res.*, 2016, **55**, 1912–1920.

131 H. Joga Rao, P. King and P. K. Yekula, Experimental investigation on adsorption of lead from aqueous solution using activated carbon from the waste rubber tire: Optimization of process parameters using central composite design, *Rasayan J. Chem.*, 2016, **9**, 254–277.

132 Y. Wei, W. Zhao, L. Xu, X. Jiang, W. Yao and Z. Shi, Research on the removal of Pb2+ from aqueous solution by electrosorption with activated carbon fibre, *Oxid. Commun.*, 2018, **41**, 296–306.

133 Z. Sui, Q. Meng, X. Zhang, R. Ma and B. Cao, Green synthesis of carbon nanotube-graphene hybrid aerogels and their use as versatile agents for water purification, *J. Mater. Chem.*, 2012, **22**, 8767–8771.

134 T. Wang, W. Liu, L. Xiong, N. Xu and J. Ni, Influence of pH, ionic strength and humic acid on competitive adsorption of Pb(II), Cd(II) and Cr(III) onto titanate nanotubes, *Chem. Eng. J.*, 2013, **215–216**, 366–374.

135 L. Yang and Z. Shi, Enhanced electrosorption capacity for lead ion removal with polypyrrole and air-plasma activated carbon nanotube composite electrode, *J. Appl. Polym. Sci.*, 2015, **132**, 41793.

136 S. Li, Y. Wei, Y. Kong, Y. Tao, C. Yao and R. Zhou, Electrochemical removal of lead ions using paper electrode of polyaniline/attapulgite composites, *Synth. Met.*, 2015, **199**, 45–50.

137 S. Majid, M. E. Rhazi, A. Amine, A. Curulli and G. Palleschi, Carbon Paste Electrode Bulk-Modified with the Conducting Polymer Poly(1,8-Diaminonaphthalene): Application to Lead Determination, *Microchim. Acta*, 2003, **143**, 195–204.

138 Y. Liao, M. Wang and D. Chen, Electrosorption of uranium(VI) by highly porous phosphate-functionalized graphene hydrogel, *Appl. Surf. Sci.*, 2019, **484**, 83–96.

139 L. Kong, M. Su, Z. Mai, H. Li, Z. Diao, Y. Xiong and D. Chen, Removal of uranium from aqueous solution by two-dimensional electrosorption reactor, *Environ. Technol. Innovation*, 2017, **8**, 57–63.

140 Y. Xu, J. W. Zondlo, H. O. Finklea and A. Brennsteiner, Electrosorption of uranium on carbon fibers as a means of environmental remediation, *Fuel Process. Technol.*, 2000, **68**, 189–208.

141 A. F. Ismail and M.-S. Yim, Investigation of activated carbon adsorbent electrode for electrosorption-based uranium extraction from seawater, *Nucl. Eng. Technol.*, 2015, **47**, 579–587.
142 S. Bao, J. Duan and Y. Zhang, Recovery of V(V) from complex vanadium solution using capacitive deionization (CDI) with resin/carbon composite electrode, *Chemosphere*, 2018, **208**, 14–20.
143 Y. Cui, S. Bao, Y. Zhang and J. Duan, Adsorption characteristics of vanadium on different resin-active carbon composite electrodes in capacitive deionization, *Chemosphere*, 2018, **212**, 34–40.
144 J. Duan, S. Bao and Y. Zhang, The characteristics of resin/carbon composite electrode and application in selective adsorption of vanadium(IV) by capacitive deionization, *Chem. Eng. Res. Des.*, 2018, **132**, 178–186.
145 C.-H. Jung, H.-Y. Lee, J.-K. Moon, H.-J. Won and Y.-G. Shul, Electrosorption of uranium ions on activated carbon fibers, *J. Radioanal. Nucl. Chem.*, 2011, **287**, 833–839.
146 C. Liu, P.-C. Hsu, J. Xie, J. Zhao, T. Wu, H. Wang, W. Liu, J. Zhang, S. Chu and Y. Cui, A half-wave rectified alternating current electrochemical method for uranium extraction from seawater, *Nat. Energy*, 2017, **2**, 17007.
147 P. S. Barber, S. P. Kelley and R. D. Rogers, Highly selective extraction of the uranyl ion with hydrophobic amidoxime-functionalized ionic liquids via η2 coordination, *RSC Adv.*, 2012, **2**, 8526–8530.
148 S. K. Ghosh, R. Saha and B. Saha, Toxicity of inorganic vanadium compounds, *Res. Chem. Intermed.*, 2015, **41**, 4873–4897.
149 J. Jiang, M. Yang, Y. Gao, J. Wang, D. Li and T. Li, Removal of toxic metals from vanadium-contaminated soils using a washing method: Reagent selection and parameter optimization, *Chemosphere*, 2017, **180**, 295–301.
150 Q. He, S. Si, J. Zhao, H. Yan, B. Sun, Q. Cai and Y. Yu, Removal of vanadium from vanadium-containing wastewater by amino modified municipal sludge derived ceramic, *Saudi J. Biol. Sci.*, 2018, **25**, 1664–1669.
151 A. Afkhami and B. E. Conway, Investigation of Removal of Cr(VI), Mo(VI), W(VI), V(IV), and V(V) Oxy-ions from Industrial Waste-Waters by Adsorption and Electrosorption at High-Area Carbon Cloth, *J. Colloid Interface Sci.*, 2002, **251**, 248–255.
152 M. Li, C. Wei, G. Fan, H. Wu, C. Li and X. Li, Acid leaching of black shale for the extraction of vanadium, *Int. J. Miner. Process.*, 2010, **95**, 62–67.
153 L. Liu, Y. Luo, W. Tan, F. Liu, S. L. Suib, Y. Zhang and G. Qiu, Zinc removal from aqueous solution using a deionization pseudocapacitor with a high-performance nanostructured birnessite electrode, *Environ. Sci.: Nano*, 2017, **4**, 811–823.
154 X. Bi, X. Feng, Y. Yang, G. Qiu, G. Li, F. Li, T. Liu, Z. Fu and Z. Jin, Environmental contamination of heavy metals from zinc smelting areas in Hezhang County, western Guizhou, China, *Environ. Int.*, 2006, **32**, 883–890.
155 W. Tang, X. Wang, G. Zeng, J. Liang, X. Li, W. Xing, D. He, L. Tang and Z. Liu, Electro-assisted Adsorption of Zn(II) on Activated Carbon Cloth in Batch-Flow Mode: Experimental and Theoretical Investigations, *Environ. Sci. Technol.*, 2019, **53**, 2670–2678.
156 H. Benakouche and M. Bounoughaz, Electrosorption Removal of the Zinc Ions from Aqueous Solution on an Artificial Electrode based in the Banana Wastes, *J. Electrochem. Sci. Technol.*, 2017, **8**, 77–86.
157 L. Liu, W. Tan, S. L. Suib, G. Qiu, L. Zheng, Q. Huang and C. Liu, Effective Zinc Adsorption Driven by Electrochemical Redox Reactions of Birnessite Nanosheets Generated by Solar Photochemistry, *ACS Sustainable Chem. Eng.*, 2018, **6**, 13907–13914.
158 G. G. Jayson, J. A. Sangster, G. Thompson and M. C. Wilkinson, Adsorption and electrosorption of mercury(II) acetate onto activated charcoal cloth from aqueous solution, *Carbon*, 1987, **25**, 523–531.
159 C. Tunsu and B. Wickman, Effective removal of mercury from aqueous streams via electrochemical alloy formation on platinum, *Nat. Commun.*, 2018, **9**, 4876.
160 H. C. Chagas, Isopotential points in the electrosorption of selenite, selenate, selenide, and tellurite at the platinum rotating disc electrode, *Can. J. Chem.*, 1979, **57**, 2560–2563.
161 E. H. Schulte and P. Scoppa, Sources and behavior of technetium in the environment, *Sci. Total Environ.*, 1987, **64**, 163–179.
162 J. Farrell, W. D. Bostick, R. J. Jarabek and J. N. Fiedor, Electrosorption and Reduction of Pertechnetate by Anodically Polarized Magnetite, *Environ. Sci. Technol.*, 1999, **33**, 1244–1249.
163 F. Kanô, I. Abe, H. Kamaya and I. Ueda, Fractal model for adsorption on activated carbon surfaces: Langmuir and Freundlich adsorption, *Surf. Sci.*, 2000, **467**, 131–138.
164 C. N. Rowe and R. W. Schiessler, Adsorption Separation Factors and Selective Adsorbent Capacities of Some Binary Liquid Hydrocarbon Mixtures1, *J. Phys. Chem.*, 1966, **70**, 787–797.
165 J. Choi, P. Dorji, H. K. Shon and S. Hong, Applications of capacitive deionization: Desalination, softening, selective removal, and energy efficiency, *Desalination*, 2019, **449**, 118–130.
166 R. Zhao, S. Porada, P. M. Biesheuvel and A. van der Wal, Energy consumption in membrane capacitive deionization for different water recoveries and flow rates, and comparison with reverse osmosis, *Desalination*, 2013, **330**, 35–41.
167 T. J. Welgemoed and C. F. Schutte, Capacitive Delonization Technology (TM) : An alternative desalination solution, *Desalination*, 2005, **183**, 327–340.
168 J. Lee, P. Srimuk, S. Carpier, J. Choi, R. L. Zornitta, C. Kim, M. Aslan and V. Presser, Confined Redox Reactions of Iodide in Carbon Nanopores for Fast and Energy-Efficient Desalination of Brackish Water and Seawater, *ChemSusChem*, 2018, **11**, 3460–3472.

